Universidade do Minho
Escola de Engenharia

Ana Rodrigues Lima

Effects of additives in artificial saliva on the corrosion and tribocorrosion behavior of cp Ti

December 22

Effects of additives in artificial saliva on the corrosion and tribocorrosion behavior of cp Ti

Ana Rodrigues Lima

UMINHO | 2022

Universidade do Minho
Escola de Engenharia

Ana Rodrigues Lima

Effects of additives in artificial saliva on the corrosion and tribocorrosion behavior of cp Ti

Master Dissertation
Integrated Master in Biomedical Engineering
Biomaterials, Rehabilitation and Biomechanics

Dissertation supervised by
Alexandra Manuela Vieira da Cruz Pinto Alves
Ana Maria Pires Pinto

December 2022

DIREITOS DE AUTOR E CONDIÇÕES DE UTILIZAÇÃO DO TRABALHO POR TERCEIROS

Este é um trabalho académico que pode ser utilizado por terceiros desde que respeitadas as regras e boas práticas internacionalmente aceites, no que concerne aos direitos de autor e direitos conexos.

Assim, o presente trabalho pode ser utilizado nos termos previstos na licença abaixo indicada.

Caso o utilizador necessite de permissão para poder fazer um uso do trabalho em condições não previstas no licenciamento indicado, deverá contactar o autor, através do RepositóriUM da Universidade do Minho.

Licença concedida aos utilizadores deste trabalho

Atribuição-NãoComercial-SemDerivações
CC BY-NC-ND

https://creativecommons.org/licenses/by-nc-nd/4.0/

Acknowledgments

First of all, I would like to thank my supervisor, Dr. Alexandra Alves, for the all the support and confidence placed in me to develop this dissertation. Your constant availability to assist and guide me were essential to both writing and laboratory work. Thank you for your patience and encouragement, and for making this experience a very enjoyable one. Thank you for your genuine concern and great advice, no matter the subject.

To my co-supervisor, Prof. Ana Pinto, for sharing your knowledge and great experience. Thank you for always having encouraging words to say and never denying assistance.

To Dr. Fatih Toptan for your help in SEM/EDS analysis and for taking time off your busy schedule to discuss my work.

To Marcelo Oliveira for your assistance in profilometry analysis.

To all the technicians for their help and great spirit, even after hours.

To all my colleagues at Lab. Functionalized Surfaces (CMEMS-UMinho), for always being ready to help and for providing great work environment.

To my friends, with a special note to Andreia, Sofia and Elisabete, for always listening to me when I needed the most and for your understanding. Thank you for always lifting me up and encourage me to be the best version of myself.

I would also like to thank my family. To my two cousins, Diogo and Rafael, for always putting a smile on my face and for being the brothers that I never had. To my godmother and my aunt for always caring and believing in me. To my grandmother and my grandfather, for your loving words and curiosity about my work, even when it was hard for you to understand.

Lastly, a special thank you to my parents, to whom I dedicate this dissertation, for your unconditional love and support throughout, not only these last few months, but all my life. I will never be able to repay you for everything you do for me. I hope this thesis make you proud.

STATEMENT OF INTEGRITY

I hereby declare having conducted this academic work with integrity. I confirm that I have not used plagiarism or any form of undue use of information or falsification of results along the process leading to its elaboration.

I further declare that I have fully acknowledged the Code of Ethical Conduct of the University of Minho.

Efeitos de aditivos na saliva artificial no comportamento à corrosão e tribocorrosão de Ti cp

RESUMO

Os implantes dentários são normalmente estruturas de Ti ou ligas de Ti colocadas na maxila ou mandíbula, para substituir as raízes dos dentes. Embora sejam bastante fiáveis, com uma taxa de sucesso de 90 a 95%, atualmente ainda são relatados casos de falha de implantes, nomeadamente devido à corrosão *in vivo* (na boca) que, além de modificar a aparência do metal exposto, pode comprometer as propriedades mecânicas do implante e causar reações adversas no organismo.

A saliva artificial Fusayama é o meio mais comum para testar o comportamento à corrosão de biomateriais dentários. O estudo do impacto de aditivos na saliva (como ácido fosfórico, PA, presente nalguns alimentos, ou ácido lático, LA, formado pelo crescimento de algumas bactérias) no comportamento à corrosão destes biomateriais é ainda escasso. Por outro lado, a tribocorrosão a que um implante dentário é sujeito está diretamente relacionada com a sua possível falha. Desta forma, o grande objetivo deste trabalho foi investigar o efeito de alguns aditivos na saliva artificial (AS) no comportamento à corrosão e tribocorrosão de Ti comercialmente puro (cp).

O melhor comportamento à corrosão do Ti cp foi em AS, tendo sido influenciado pela presença de aditivos. O aumento do teor de LA (2,5 e 5 g/L) teve efeito negligenciável no comportamento à corrosão, no entanto, quando adicionadas diferentes concentrações de PA (1 e 14 M), o comportamento à corrosão do Ti cp piorou, verificando-se que ocorreu um aumento tanto da suscetibilidade como da taxa de corrosão. Em condições tribo-eletroquímicas, os papéis inverteram-se. Ao OCP, quando em contacto com AS, o filme passivo formado na superfície do Ti cp, juntamente com os produtos de desgaste resultantes do contacto mecânico, promoveram menor proteção ao material, o que levou à formação de pistas de desgaste de maiores dimensões e, deste modo, um volume de desgaste superior. Ao adicionar LA, o desgaste do material foi ligeiramente, mas não consideravelmente, menor. Por outro lado, a adição de PA, devido à presença de fósforo (P), um constituinte de lubrificantes industriais, levou a um desgaste menor. Os mecanismos de tribocorrosão consistiram em mecanismos de abrasão e adesão, porém, foi detetada fadiga quando o PA 14M foi adicionado. Nos ensaios potenciostáticos ($+0,5V_{Ag/AgCl}$) concluiu-se que, no caso da AS, o desgaste mecânico foi dominante. Já com a adição de aditivos, a corrosão foi significativa, confirmando um sinergismo entre corrosão e desgaste.

Palavras-chave: aditivos, corrosão, saliva artificial Fusayama, Ti cp, tribocorrosão.

Effects of additives in artificial saliva on the corrosion and tribocorrosion behavior of cp Ti

ABSTRACT

Dental implants, which are usually made of Ti or its alloys, are placed in the maxilla or mandible to replace the roots of the teeth. Although they are quite reliable, with a 10-year success rate of 90 to 95%, nowadays, cases of implant failure are still reported, namely due to *in vivo* corrosion (in the mouth). This phenomenon, in addition to modifying the appearance of the exposed metal, can compromise the mechanical properties of the implant and cause adverse reactions in the body.

Fusayama´s artificial saliva is the most common testing solution to access the corrosion behavior of dental biomaterials. However, the impact of additives in saliva (such as phosphoric acid, PA, found in some foods, or lactic acid, LA, formed by the growth of bacteria) on the corrosion behavior of these biomaterials is still scarce. On the other hand, tribocorrosion effect on a dental implant is directly related to its possible failure. Hence, the main goal of this work was to study the effect of some additives, at different concentrations, in artificial saliva (AS) on the corrosion and tribocorrosion behavior of cp Ti.

Cp Ti best corrosion behavior was promoted by AS, and significantly influenced by the presence of additives. Increasing amount of LA (2.5 and 5 g/L) had negligible effect on corrosion behavior, however, the added different concentrations PA (1 and 14 M) were detrimental for both corrosion susceptibility and rate. In tribo-electrochemical conditions, the roles reversed. At OCP, in AS, the passive film formed on cp Ti surface, along with the wear debris resulting from the mechanical contact, promoted the lowest level of protection to the material, leading to the largest wear tracks and, therefore, the highest volume loss. By adding LA, the mechanical damage was slightly lower, but not considerable. On the other hand, the addition of PA, due to the presence of P, a known constituent of industrial lubricants, leaded to the smallest wear tracks. The tribocorrosion mechanisms consisted in abrasion and adhesion mechanisms, however, fatigue phenomenon was detected when PA 14M was added. In potentiostatic conditions ($+0.5V_{Ag/AgCl}$) it was concluided that, in the case of AS, mechanical wear was dominant, and when additives were added, corrosion was significant, confirming a synergism between corrosion and wear.

Keywords: additives, cp Ti, corrosion, Fusayama´s artificial saliva, tribocorrosion.

Table of Contents

List of Figures

List of Tables

List of Abbreviations and acronyms

A

AS	Artificial Saliva
ASTM	American Society for Testing and Materials

B

BSE	Backscattered Electrons

C

CE	Counter Electrode
COF	Coefficient Of Friction
CP	Commercially Pure
CPE	Constant Phase Element

E

$E_{(i=0)}$	Corrosion Potential
EDS	Energy Dispersive Spectroscopy
EEC	Electrical Equivalent Circuit
EFC	European Federation of Corrosion
EIS	Electrochemical Impedance Spectroscopy

F

FAS	Fusayama's Artificial Saliva

H

HV	Vickers Hardness

I

i_c	Critical Current Density
i_{pass}	Passivation Current Density

L

LA	Lactic Acid

O

OCP	Open-Circuit Potential

OM Optical Microscopy

P

PA Phosphoric Acid

PDP Potentiodynamic Polarization

R

RE Reference Electrode

S

SCE Saturated Calomel Electrode

SE Secondary Electrons

SEM Scanning Electron Microscopy

U

UTS Ultimate Tensile Strength

W

WE Working Electrode

X

XPS X-ray Photoelectron Spectroscopy

Y

YS Yield Strength

1 GENERAL INTRODUCTION

Nowadays people are starting to become more aware of the importance of watching over their health, and they are starting to prioritize dental care, in order to improve their life quality. Although studies are paying more attention to technicalities that can actually make a difference on the implants' durability and reliability, the research for the perfect dental implant is still ongoing. The human body is complex and somehow still unknown, especially when it comes to the oral cavity environment and how it affects the material incorporated on the implanted devices.

1.1 CONTEXT AND MOTIVATION

Implantology is an area of dentistry that involves the entry and placement of dental implants, as well as the associated surgical procedures [1]. As shown in Figure 1, these dental implants are, generally, composed by a ceramic crown attached to a metallic screw (frequently made of Ti), placed in the maxilla or mandible, which replaces the roots of the teeth. These structures are mostly needed due to edentulislm (condition where some or all teeth are missing), caused by periodontal disease (caused by bacteria), caries or injury [2–4]. Also, implants offer total prosthesis stability while avoiding damage to any of the remaining natural teeth [3].

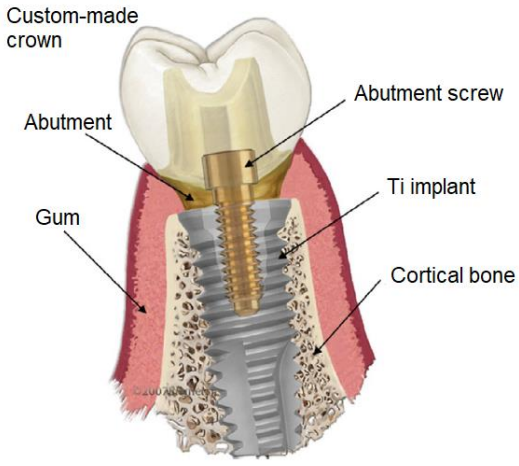

Figure 1 - Schematic representation of a dental implant. Adapted from [3].

According to the Institute of Implantology, although the Portuguese have been paying more and more attention to oral health, 27% of the Portuguese population have never had access to consultations with a dentist and/or stomatologist and about 68% have lack natural teeth, which leads to chewing quality loss and self-esteem problems [5].

Thus, the clinical demand for optimized, personalized, comfortable treatment solutions that, at the same time, maintain dental function and aesthetics has been growing exponentially, leading to the enormous challenge: finding the perfect implant. Despite the indisputable evolution in this field, there is still a long way to go, as cases of dental implant failure are still reported. The main cause of failure is *in vivo* corrosion, in mouth. This can result in the release of potentially toxic corrosion products, which, in addition to modifying the appearance and topography of the exposed metallic implant, it can compromise its mechanical properties. In these cases, removal surgery is necessary, which is sometimes very painful to the patients, whose recovery takes time [6].

The driving force for corrosion in the oral cavity is the saliva, as this is the environment where everything is triggered. Hence, its constitution, as well as its constant change (for example, due to eating and hygiene habits or diseases) and the dynamic environment that is generated are some of the main factors to be taken into consideration when studying corrosion in dental prostheses. Fusayama´s artificial saliva (FAS) [7] is the most common medium to test the corrosion behavior of biomaterials used in dentistry. Nevertheless, there is a gap in the literature regarding the effect of some additives in the saliva, such as phosphoric acid (present in some foods) or lactic acid (which can be formed by the growth of some bacteria), on the corrosion behavior of these biomaterials. On the other hand, the tribocorrosion, defined as the combined action of corrosion and wear (caused by chewing and talking movements), to which a dental implant is subjected is directly related to its possible functionality loss.

It is also important to note that, when designing a dental implant, the material selection is a fundamental decision for the precision and predictability of the treatment. For years, precious metals, such as gold, were used, as they are less susceptible to corrosion. However, they are more expensive and have insufficient mechanical properties, which has raised interest in finding cheaper metals without a major compromise of the metal's corrosion stability [8]. For example, Ti, due to its mechanical behavior, good resistance to corrosion in the presence of body fluids and nontoxicity, is widely used in dental implants these days [3,6]. Although it is commonly used as the major component of alloys, its commercially pure form (cp Ti) is frequently used, so it is going to be the topic of discussion on the present investigation.

1.2 OBJECTIVES AND HYPOTHESIS

The objective of this dissertation was to study the effect of additives in artificial saliva in the corrosion and tribocrrosion mechanisms of cp Ti.

Hence, the hypothesis of this work is that the presence of additives in artificial saliva influences corrosion and tribocorrosion behavior of cp Ti.

1.3 STRUCTURE OF THE DISSERTATION

This thesis is structured in 5 chapters. The first chapter provides a general introduction on the topic, as well as the context, motivation and objectives of this work.

In chapter 2 is presented the state of the art, where some relevant theoretical concepts and technologies are addressed. Additionally, this chapter includes a literature review by referencing and discussing studies on the effect of some additives in FAS on the corrosion and tribocorrosion behavior of cp Ti.

Chapter 3 describes the materials and methods used for the preparation of the cp Ti samples and the electrolytes, as well as for the electrochemical and tribo-electrochemical tests and characterization techniques.

In chapter 4, the results are compiled and discussed in order to compare all the conditions for electrochemical and tribo-electrochemical tests.

Finally, in chapter 5, the conclusions are presented, as well as future works that can complete this study even more and provide important information to promote an even greater development of optimized dental implants.

2 STATE OF THE ART

As mentioned before, with the scientific and technological advances of the 20th century, there is an increasing awareness about dental care being one of the keys to a healthy life. At the same time, the demand for implants to replace natural teeth is growing, as it is estimated that, each year, devices like this are implanted in approximately 275 000 people, all over the world, with some patients needing more than 12 implants [6].

When it comes to dental implants, the conditions they are subjected to are conducive to causing unwanted reactions, especially on the metallic screw (which mimics the root of teeth), that fits into the ceramic crown, mainly because it contacts directly with the adjacent tissues, either gum or bone. This screw, whose material should exhibit similar properties to the bone, is often made of Ti, since it is reported as a passive metal that best behaves in physiological environment, in this case, mouth [3,6].

The saliva constitution is continuously changing due to several external and/or internal factors. In this way, besides saliva basic components, some additives can be found, altering its pH. To this extent, when choosing a material that is meant to be inserted in the human body, along with some specific chemical and mechanical properties, nontoxicity and good corrosion resistance are primary requirements [3,9,10].

Thereby, studying the corrosion behavior of metallic implants is of extreme importance because it can cause an unfavorable impact on its biocompatibility (due to the release of metallic ions that can cause an adverse reaction in connective or epithelial tissues), mechanical integrity and osseointegration, promoting the device deficiency and, consequently, its failure. On the other hand, it is not just about the corrosion mechanisms. The implants failure is usually determined by the dynamic environment that is the human mouth and its influence on the chosen material, due to biomechanical (wear) and biochemical (corrosion) phenomena occurring simultaneously, meaning that a complex tribocorrosion system is generated [6].

Nonetheless, it is important to point that this synergism between wear and corrosion may disturb or, sometimes in more severe conditions or long-term exposure, destruct the protective film formed on the surface. In this way it is imperishable to understand the recurring depassivation and repassivation and how this cyclic behavior is related to different additives detected in the saliva [11].

2.1 DENTAL STRUCTURE

Before addressing the central topics of this dissertation, it is important to know the constitution of the teeth, as well as some relevant orofacial structures.

The oral cavity is the "heart" of the orofacial system, as it is where all the teeth are located. An average adult possesses 32 permanent teeth, while each quadrant of the cavity has two incisors, one canine, two premolars and three molars [12]. As illustrated in Figure 2, dental structure consists in three hard components: dentin, enamel and cement (or cementum) [11,12].

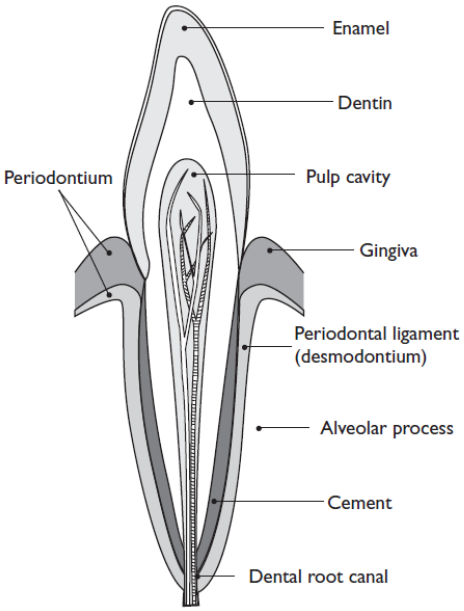

Figure 2 - Schematic representation of a sagittal section through a tooth, showing major its anatomic components [12].

Dentin is part of the tooth bulk and is essentially needed to provide support and stress distribution [13]. Like bone, dentin is a hydrated biological composite structure formed by a matrix of collagen type I (around 92%; produced by odontoblasts, located in the dentin/enamel margin) reinforced with a calcium phosphate mineral, called apatite [11,12]. As shown in Table 2, dentin (80 to 92 HV) is harder than the cortical bone (43 to 76 HV) due to its higher inorganic composition [13]. When compared to the enamel, dentin is more porous and has higher organic phase (about 21%) [13]. Furthermore, it is reported that its flexibility might help prevent the fracture of enamel, which is characterized for its brittleness [12,13].

The dentin root is covered by cement. This cement is anchored to a fibrous joint, called periodontal ligament, which provides a connection between the tooth and the alveolar bone [12].

Enamel (with thickness up to 2 mm) is the hardest substance in the human body, with 300 to 410 HV, and it consists in the outer layer of the tooth, as it coats and protects the dentin, allowing efficient

mastication. Mature enamel is a crystalline structure, as it is highly calcified. Its composition consists in 96 wt.% inorganic material (mineral), 1 wt.% lipids and proteins, and the rest being water [11,13]. The cells responsible for enamel production are located in the outer surface of the enamel and are quickly worn out as teeth growth happens. Enamel damage cases, also known as caries, are quite frequent, however it does not possess regenerative capacity [12].

Caries are developed basically due to mineral dissolution. Generally, teeth demineralization is motivated by acids (lactic, acetic, propionic, among others) expelled by bacteria, as a result of the metabolism of carbohydrates [13]. In dental implant-supported prosthesis, bacteria accumulate on top of the dental pellicle (protein film, formed almost instantaneously after the contact with saliva, which protects the tooth from those acids) on the tooth surface and colonize existing gaps between teeth, forming "plaque". For example, between the implant and the abutment (see Figure 4), gaps of 2.5 to 60 μm were reported, and as the microorganisms' diameter is under 10 μm, these prosthetic gaps can be effortlessly colonized by several microorganisms [10]. Thus, microgaps are the most susceptible areas for biofilm formation, which will strongly affect corrosion and tribocorrosion mechanisms.

These colonies, also known as oral biofilms, are defined as "*a population of microbes associated with extracellular polymers forming at an interface*" [13], and can be more that 1 mm thick. Although the ingestion of acidic foods or drinks can also damage the teeth and cause the loss from enamel, bacteria (simple anucleated cells) is still the number one cause of caries. Also, it is important to note that, besides tooth decay, 100% of gingivitis cases are directly linked to biofilms formation [13].

All biomaterials used in oral restoration are prone to biofilm formation and proliferation and consequent events like epithelium downgrowth and bone loss around the implant often lead to implant failure [11]. In this way, pathological conditions of the tissues around dental implants, such as peri-implantitis may happen, and they are commonly related with the same bacteria (*A. actinomycetemcomitans*) as periodontitis, however, the dental implant material role is not yet clarified [11,14,15].

It is imperative that the chosen materials are relatively similar to the structures described above [11]. Ti is one of the most used biomaterials in dental implants. It is reported that the bonds between Ti implants and the epithelium are morphologically similar to the original bond with the tooth, however, this interface has not been fully characterized. On the other hand, although connective tissue does not bond with Ti, it is able to form a tight seal that reduces bacteria migration, as well as the deposition of their metabolites [11]. Thus, many materials frequently used in dental implantology were organized by Berry *et al.* [16] in a descending order according to its antibacterial activity: Au > Ti > Co > V > Al > Cr > Fe.

2.2 DENTAL IMPLANTS

Dental implants history goes way back to the Ancient Egyptian civilization (3000 B.C.) where the first Cu stud was applied inside the mouth [6]. Replacing the missing teeth in earlier times included natural materials such as bamboo pegs, animal or human teeth, seashells and ivory, and even sometimes, stones [3]. The years went by and countless diverse attempts to replace missing teeth were made in order to regain full, comfortable masticatory function and facial aesthetics, but nothing seemed to be working, at least on the long-term. Until 1809, when a French dentist, Maggiolo J., described the implantation process of a gold alloy with three branches into the jawbone, and the installation of a porcelain crown [17].

In the early 1900s the metallic artificial root forms commonly resorted for tooth functionality restoration [3]. In 1937, new materials were found to be effective, CoCrMo alloy was developed and implanted by Stock at Harvard University. Later in 1940, Dahl presented a revolutionary approach, by being the first person to attempt subperiosteal implant [17].

In 1969, the term "osseointegration" was presented by Per-Ingvar Brånemark and his colleagues, as "*a direct structural and functional connection between ordered, living bone and the surface of a load-carrying implant*" [3]. Brånemark and his co-workers were studying the microcirculation of blood around a cp Ti implant in a rabbit, and they realized that it was hard to remove the device, since bone has grown and deposit around it, leading to its osseointegration. Thus, Dr. Brånemark developed a root form threaded Ti implant to use in his patients [3,17]. Another historical mark was made by Dr. Lee, who introduced an endosseous implant with a central post. In the 1960s, other great discoveries were made, since Dr. Leonard Linkow proposed the newly updated version of the basic spiral design, the blade implant (endosseous), and made it possible to use in either the maxilla or mandible [17].

In 1963, the first screw-type implant (*Ventplant*) was finalized. At first it was made of a CoCr alloy, but it was replaced by Ti due to Brånemark's investigation. Brånemark's concept expanded rapidly throughout the decades and still is the keystone of today's newest implants [2,17]. Another key and historical fact to highlight is related to Scharf and Tarnow's [18] publication, in 1993, regarding some data that showed high success rate implantations in a dental office setting under aseptic conditions. This was a big step forward as surgery room setups are more expensive than a regular dental office equipment.

These days, computer aided design and manufacturing technologies are used to conceive prostheses which mimic the patients' natural teeth and capable of withstanding similar loads. Plus, zirconia has started to appear as an alternative to Ti, as it is reported that it provides better integration and response from the adjacent tissues, however "*further clinical studies are needed before such*

recommendation, as it remains a brittle ceramic material with a significant sensitivity to surface defects" [17,19].

2.2.1 TYPES OF DENTAL IMPLANTS

There are two types of dental implants: endosteal (also called endosseous) and subperiosteal. The endosteal type is in direct contact with bone tissue, and has different available shapes and forms, such as root form (screws), blades (plates), transosseous, among others. On the other hand, the subperiosteal type are placed along the bone surfaces, under the periosteum (membrane that covers the outer surface of all bones), conducting every tension to the cortical bone [2,6,20,21]. In Figure 3 it is possible to observe different dental implant types.

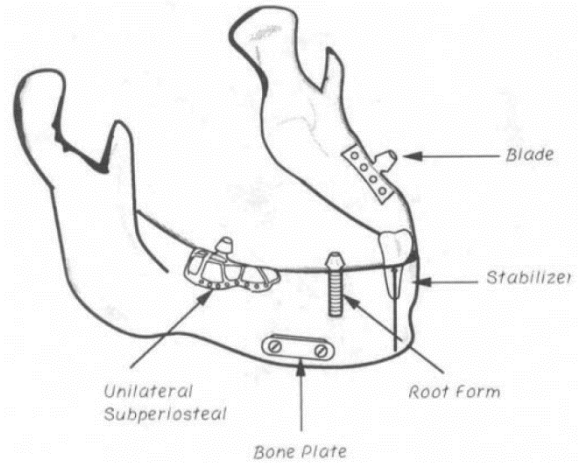

Figure 3 - Schematic representation of different dental implant designs [6].

In this dissertation, the focus is on endosseous implants like the one in Figure 4, (specifically on the screw) since they are the most common and problematic type, essentially due to its invasiveness. These implants are normally cylindrical and consist in an artificial tooth surgically anchored to the mandible or maxilla and are part of a three-component system. There is an abutment that connects the ceramic crown to the metallic screw (the "anchor"), normally made of Ti [6].

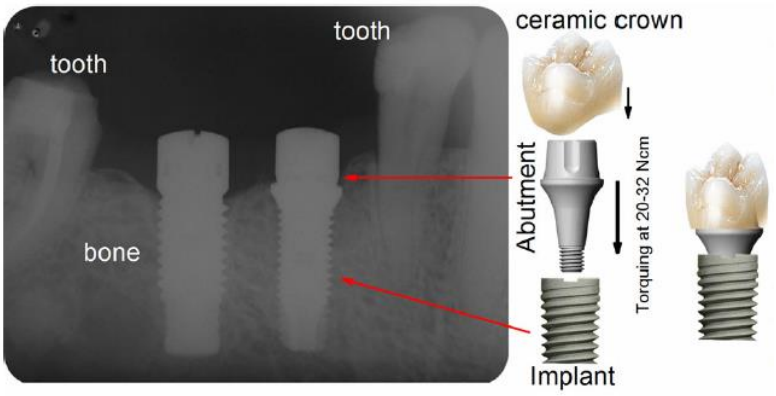

Figure 4 - Schematic structure of an endosseous dental implant, and its components [10].

2.2.2 BIOMATERIALS IN ENDOSSEOUS DENTAL IMPLANTS

First and foremost, the term biomaterial is continuously changing by the years. Even so, as proposed by the Biomaterials journal, biomaterial is defined as *"a substance that has been engineered to take form, which, alone or as a part of a complex system, is used to direct, by control of interactions with components of living systems, the course of any therapeutic or diagnostic procedure"* [22]. There are four major biomaterial categories: metals, polymers, ceramics and their composites.

Ancient civilizations, such as the Romans, Chinese and Aztec, used Au in dentistry. Since then, precious metals were widely used to ensure minimal corrosion. However, in nowadays the search for cheaper and more efficient materials became mandatory [6].

In the 60's and 70's, ceramics like alumina, hydroxyapatite and tricalcium phosphate were first used, however, despite presenting a good biological response, their brittleness is a big disadvantage on load-bearing applications like dental implants. On the other hand, polymers have also been used before due to their easier manufacturing ability, but their poor mechanical and biological response have restrained their application [23].

In the orthodontic field, when it comes to the placement of endosseous implants, the ambition is to have an osseo- and bio-integrated structure. Many biomaterials have been used, but just a few have proven to be effective long-term, considering the cyclic loads that the implants are subjected. Thereby, metals are probably the oldest type of biomaterials used for dental prostheses and, by far, the most frequently used on nowadays threaded implants, because of its high mechanical strength and integrity. Precious metals, stainless steel, tantalum and Co-Cr alloys were incorporated to these implants screw, but Ti introduction changed the course of dental implantology history, due to its better acceptance in the body and, also, it is able to be properly integrated with the bone [6,17,23,24].

2.3 CP TI IN THE ORTHODONTIC FIELD

Souza *et al.* [10] stated that *"a dental implant-supported prosthesis should possess mechanical properties similar to the dental and bone structures in order to establish a long-term clinical performance and harmony with the masticatory system"* and, as stated before, choosing the right material is perhaps the most important step to achieve it.

Biocompatibility is a top requirement when choosing a material to incorporate in dental implants, as it has been defined, according to Williams [23] as "*the ability of a material to perform with an appropriate host response in a specific application*", and it covers all aspects of the interactions between the material and tissues. If there is any sort of evidence of degradation the adjacent tissues to the implant, the material is considered toxic and, therefore, non-biocompatible.

Therefore, an ideal implant material should be, primary, biocompatible, but basic mechanical properties such as hardness, ductility, yield strength and Young's modulus are important to choose a material. Physical and chemical properties of the materials (bulk and surface) are determinant factors to the corrosion and tribocorrosion mechanism and, thus, to the clinical success and prediction of implant therapy as well. Not only is important to have full knowledge about these properties, but also how they are interrelated with the constitution, microstructure and crystallographic components of the phases, their ratio, distribution and orientation [6,25].

Since the clinical success of Brånemark's research, Ti has been widely discussed by many authors, being the material of choice for the fabrication of root-form implants to support the oral prosthesis (Figure 4), due to its great mechanical properties (almost equal that of nigh noble alloys, at much lower price), biocompatibility and high corrosion resistance [2,6,11,17,26].

2.3.1 PROPERTIES OF CP TI

Cp Ti is one of the most common biomaterials to be incorporated in these units, mainly due to its low density, attractive mechanical properties (compared to, for example, highly used in the past, titanium alloy Ti-6Al-4V - Table 1), such as relatively low Young's modulus, low toxicity, ability to be osseointegrated and great corrosion resistance when in contact with body fluids, such as saliva [3,6,27].

Ti-based alloys have two allotropic structures (Figure 5): hexagonal close-packed (HCP), called α phase, up to 882°C, and body-centered cubic (BCC), also known as β phase, above the previous temperature. Therefore, Ti-based alloys can be known as α, $\alpha + \beta$ or β [3,6,11,28].

Cp Ti exists in a hexagonal close-packed (HCP) structure, called α phase, at room temperature (25°C), and is an unalloyed Ti, available in four ASTM F67 grades: 1, 2, 3 and 4. These grades differ on slight variations in the percentages of residual elements such as N, C, H, Fe, O, as shown in Table 1, which generates different mechanical and physical properties, for each grade (Table 2). The reason for this range of properties essentially resides in the oxygen content, since it is the predominant element after titanium (about 99%), however, as investigated by González *et al.* [27], the effect of the remaining elements should not be underestimated [3,29].

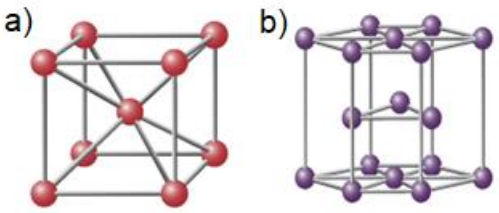

Figure 5 - Titanium crystal lattice unit cells: (a) body-centered cubic cell, and (b) hexagonal close-packed. Adapted from [11].

On the other hand, Ti-6Al-4V, also known as Ti64 or ASTM F136 (grade 5), is an α + β alloy: the addition of Al, an α-phase stabilizer that decreases its density while increasing its strength, and vanadium (V), a β-phase stabilizer, to the elements listed for pure titanium. This combination of phases also provides higher strength to the alloy and better wear resistance [6,30,31]. This alloy was used in the past, but not as much anymore due to toxicity concerns about V [6]. González *et al.* [27] also concluded that al enrichment of the α-phase, in this case, Al, was found to be detrimental to the passivity and corrosion resistance of Ti.

Both, specific weight (4.5 g/cm^3) and Young's modulus (also known as, elasticity modulus, stiffness or rigidity) of cp Ti are independent of the grade (103 to 107 GPa) [32]. The Young's modulus is similar to the Ti-6Al-4V alloy (110 to 114 GPa), however, five to six times higher than the cortical bone. It is important that the material Young's modulus matches, or it is not too high compared to the cortical bone (10 to 18 GPa), so that the stress transfer between the dental implant and the bone is well distributed. Otherwise, stress shielding occurs. This well-known phenomenon that consists in the transfer of all the loads to the implant, protects the bone. This way, the bone tissue is protected/shielded, leading to bone atrophy and, possibly, its resorption and necrosis may occur. Consequently, the implant can become loose, meaning that its clinical failure is inevitable [25,32,33].

It is reported that the oxygen ratio increases both yield strength (YS) and ultimate tensile strength (UTS), and decrease ductility [3,6,32]. At atomic level, oxygen atoms take up room as they dissolve into

the crystal lattice as interstitial atoms, squeezing Ti ions. Thus, higher oxygen content leads to less movements within the lattice, which means lower ductility [30].

For example, in cp Ti grade 1, at 0.18 at. % oxygen, the YS and UTS are, respectively, around 170 MPa and 240 MPa, while, in grade 4 (0.40% oxygen), these properties increase to 483 MPa and 550 MPa, respectively. Additionally, Ti-6Al-4V exhibits even greater UTS than grade 4 (860 MPa).

For metallic materials, hardness is one of the most important parameters, since it is an indicator of the Ti wear resistance. It is a critical property given the occlusal loads (cyclic loads instigated by tooth against tooth movements during mastication). Harder metals are usually less prone to suffering damages when subjected to a tribocorrosive environment, but, on the other hand, they are less ductile and tough, which is not exactly desirable given the mechanical loads which dental implants are subjected [11].

To be noted that hardness and YS are, somehow, related. Usually, metals with higher values of hardness also present high YS, which means they are harder to scratch/polish. In dentals applications, the enamel hardness must be lower than the material's, otherwise the enamel might be worn out by the metallic material. This phenomenon is undesirable because, when combined with the oral environment, it might get worse, jeopardizing the clinical success of the implant. As shown in Table 2, enamel exhibits significantly higher Vickers hardness than all cp Ti grades and alloy [11].

Moreover, cp Ti grade 1 presents the best corrosion resistance. Besides, since it has the lowest oxygen percentage presents the lowest strength and highest ductility at room temperature, meaning that it is the easiest to be cold-worked. On the other hand, cp Ti grade 2 possesses similar great corrosion behavior and biocompatibility when compared to cp Ti grade 1, however, it exhibits higher YS and UTS, which is great for bending resistance, but not too high to the point of not being compatible with bone. Because of this great property compromise, grade 2 is the main cp Ti incorporated in dental implant applications [29,33–35]. And finally, grades 3 and 4 are more resistant (with higher YS and UTS), being that grade 4, due to its highest oxygen ratio of all four ASTM grades, is mechanically the strongest and less ductile. In both cases, YS and UTS make them relatively incompatible with the cortical bone, and, therefore, not adequate to dental implant applications [29].

Table 1 - Elemental composition of cp Ti (grades 1, 2, 3 and 4) and Ti-6Al-4V alloy. Adapted from [6,32].

Element (%)	Cp Ti Grade 1	Cp Ti Grade 2	Cp Ti Grade 3	Cp Ti Grade 4	Ti-6Al-4V
Nitrogen (N)	0.03	0.03	0.05	0.05	0.05
Carbon (C)	0.10	0.10	0.10	0.10	0.08
Hydrogen (H)	0.015	0.015	0.015	0.015	0.012
Iron (Fe)	0.02	0.03	0.03	0.05	0.25
Oxygen (O)	0.18	0.25	0.35	0.40	0.13
Aluminum (Al)	–	–	–	–	5.5-6.5
Vanadium (V)	–	–	–	–	3.5-4.5
Titanium (Ti)	Balance	Balance	Balance	Balance	88.3-90.8

Table 2 - Mechanical properties of Cp Ti (grades 1, 2, 3 and 4), Ti-6Al-4V, cortical bone, dentin and enamel. Adapted from [3,6,10,11,31,32].

Material	Ultimate Tensile Strength (MPa)	Yield Strength (MPa)	Elongation (%)	Young's Modulus (GPa)	Specific Weight (g/cm^3)	Vickers Hardness (HV)
Cp Ti Grade 1	240	170	24	103-107	4.5	120- 150
Cp Ti Grade 2	345	275	20	103-107	4.5	180-209
Cp Ti Grade 3	450	380	18	103-107	4.5	190-240
Cp Ti Grade 4	550	483	15	103-107	4.5	280
Ti-6Al-4V (Grade 5)	862	793	10	114-120	4.4	350
Cortical bone	140	30-70	0-8	10-18	0.7	43-76
Dentin	52	–	–	11-19	2.1	80-92
Enamel	10	–	–	75-100	2.96	300-410

2.3.2 PASSIVATION OF TI

It is reported titanium has low corrosion rate in corrosive environments, as the oral cavity, derives from its passive behavior, by growing a strongly adherent oxide film on its surface (Figure 6), when in the presence of oxygen [3,4,11,28,36]. Because of this protective layer, when exposed to saliva, Ti manages to retain this outer surface layer and, thus, keep its attractive mechanical and toxicological properties, which dictates its extensive use and study in dental implantology (especially Cp Ti grade 2, as mentioned before).

Cp Ti is well known to be tolerated in the human body because it can spontaneously react with the surrounding media and form an oxide layer which has a protective function, as it prevents material-medium interactions. This passive barrier (typically 3 to 7 nm, but can go up to 10 nm) is commonly an amorphous layer of n-semiconducting titanium dioxide, TiO_2 ($Ti^{4+} + 2O^{2-}$), with the ability to control cp Ti corrosion behavior, as it acts like a barrier to chemical attack. Usually, these films are amorphous, however, depending on the conditions where it was established, anatase and rutile nanocrystals could be found [28,35]. The Ti_2O/Ti has, approximately, a 2:1 ratio and it gradually reduces from as it approaches to the bulk. Moreover, hydroxides and chemisorbed water can also bond with Ti^{4+} [4].

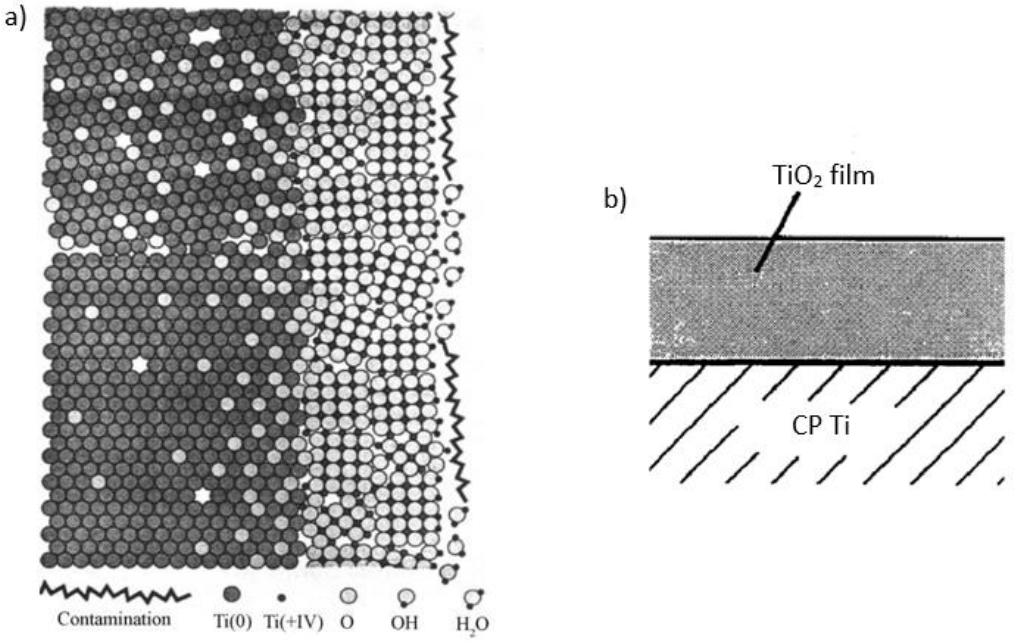

Figure 6 - Schematic representation of (a) the formation of oxide film formed on cp Ti, at room temperature, and (b) the TiO2 layer. Adapted from [4,27].

This oxide outer layer and its dissolution products seem to be biologically inert, meaning they do not induce allergic or inflammatory reactions in adjacent tissues [4,34]. However, even in its passive state, chemical dissolution happens and ions are released from the oxide film, which means Ti is not entirely

inert. As an advantage, this almost inertness allows bone growth and the osseointegration of the implant [11].

There is *in vivo* evidence that even greater corrosion behavior can be developed by a thicker film [34]. Besides the thickness of the layer, its physical and electrochemical properties, which depend on the metallic bulk nature and the surrounding environment, are determinant for Ti stability and degree of passivity [27].

As observed in Ti Pourbaix diagram (Figure 7), besides the most common oxide, TiO_2, other several oxide stoichiometries can be generated, in water, for different pH ranges: TiO, Ti_2O_3 and TiO_3. By analyzing the potential/pH diagram, the passive area is notoriously large, indicating passive films stability through a broad range of pH and potential values. Additionally, there are many Ti species (Ti, Ti^{2+}, Ti^{3+}, TiO, TiO_2, Ti_2O_3 and $TiO_3 \cdot 2H_2O$) that are stable for specific conditions [37,38].

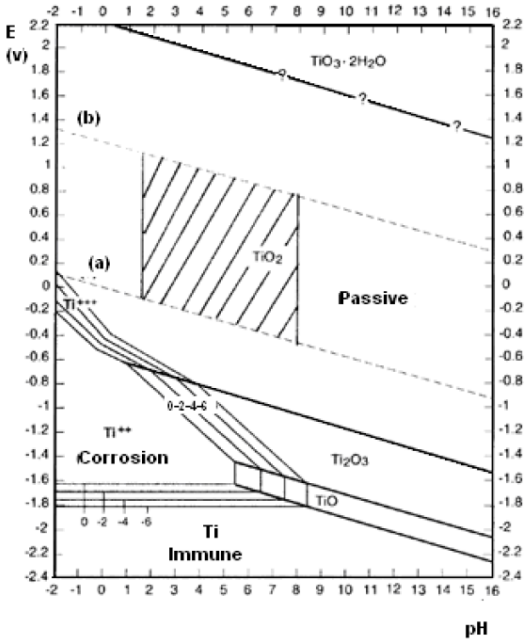

Figure 7 - Pourbaix diagram of titanium in water, at 25°C [38].

In typical physiological conditions (saliva normal pH is 6 to 7), Ti is in its passive state but, as the conditions in the oral cavity can change, and certain substances can be produced by the body or ingested, breakdown of passivity can happen [10,11]. However, when the film is disturbed, Ti can instantly repassivate, thanks to the "*surface oxidation-controlled kinetics*" (Sakaguchi *et al.* [11]), and form a new compact film, getting back the well-known excellent biocompatibility and corrosion resistance.

Simultaneously to electrochemical reactions (corrosion), friction and sliding-wear happen during occlusal movements, leading to the oxide film detachment and even further dissolution as more potentially toxic ions added to the environment. This compromises the implants viability and clinical success [35].

2.4 SURFACE CHARACTERISTICS AND ITS INFLUENCE ON THE IMPLANTS OSSEOINTEGRATION

Surface properties of an endosseous implant impacts the osseointegration process. In the past, implant surfaces were categorized as rough or smooth, however, nowadays, surfaces are more complex, so that, when proposing an implant, in order to promote the desirable bone formation around the implant and, consequently, reduce the healing time, factors such as the chemistry, geometry and topography of the materials surface must be taken into consideration by the engineer [3,37]. This osseointegrative mechanism includes protein absorption, platelet interactions and activation, signaling molecules, and osteogenic cell migration and differentiation [3].

Topography has great influence on the implants osseointegration capacity, perhaps even greater influence than corrosion and tribocorrosion behavior of the materials [3,37]. Some studies have been conducted to improve surface architecture of Ti implants [39–42]. It is reported that surface designs with undercuts and/or slightly porous provide to the implant remarkably higher mechanical interlocking with bone. Lower scale features (for example, micro or nanometric levels) earlier bone deposition, while slightly higher scales impact late/intermediate integration with anchoring points for the collagen of the newly formed bone [3,37]. As a result, a surface with different scales features is desirable in order to take advantage of both effects, and thus have a continuous osseointegration process of the implant [3].

As will be further addressed, corrosion, either by itself, or accompanied with mastication and/or occlusal forces can lead to surface damage of the implant. Whenever two surfaces rub against each other in a corrosive environment (either implant/implant or implant/tooth), Ti passive film is removed, which means that the fresh metal is exposed. The fresh metal is less stable and more prone to chemical and mechanical attack, compared to the removed film, since it did not go through the process of interacting and reacting with the surrounding environment. As the film is removed, chemical and physical properties of Ti surface change since it is no longer protected, which leads to surface corrosion and release of metallic ions and debris into the oral cavity, which might be harmful and toxic [37].

2.5 THE ORAL ENVIRONMENT

Biocompatibility of a dental material depends on its composition, location, and interactions with the oral cavity [11]. Overall, the physiological environment is complex and severe, which can accelerate and exacerbate biomaterials degradation. More specifically, when a device/material is inserted in the mouth, it is subjected to biochemical and biological actions and instantly contacts with saliva. Besides saliva, it is also crucial to know the teeth and its constituents, as well as masticatory forces and what could be eventually causing teeth loss.

2.5.1 SALIVA AS AN ELECTROLYTE

Human saliva (pH 6 to 7) is the body fluid that abounds the oral cavity and consists in a cocktail of water (about 99 vol.%) and biochemical, organic and inorganic substances produced by three pairs of salivary glands (parotid, submaxilar and submandibular) and the oral mucosal glands (labial, lingual, palatal, and vestibular) [10,43].

The organic compounds consist in a variety of important proteins (albumin, proline-rich proteins, statherin, histatin, etc.), glycoproteins (mucin), characterized by providing the viscosity to saliva, and aminoacids (leucine, glycine, glutamate, aspartate) for the oral health, with specific biological functions [10,37]. Additionally, carbohydrates (glucose, galactosis, sialic acid), lipids (phospholipids, triglycerides and cholesterol), and antibodies (IgAs, IgM, IgG) and enzymes (lyzozyme, lactoferrin, lactoperoxidase), which are responsible for the elimination of microorganisms, are organic constituents as well. On the other hand, saliva inorganic compounds are basically consisting in ions like Ca^{2+}, PO_4^{3-}, Na^{+}, K^{+} and HCO^{3-}, being that bicarbonate (HCO^{3-}) and phosphate (PO_4^{3-}) ions act as buffers to preserve the saliva normal pH values [44]. Bicarbonate ionic bond to H^{+}, forming H_2CO_3, H_2 and CO_2, is the main buffering mechanism, since it is responsible to increase saliva´s pH, leading to prevention of teeth demineralization. On the other hand, this process can be jeopardized if there is of microbial cells density or low salivary flow rate [44,45].

It is important to note that saliva plays a fundamental role in human life in general. It is a key element to regulate microbial colonization on oral tissues, breakdown food by lubricating the mouth, as well as assisting the swallowing motions and the digestive process, and cleaning the oral cavity [43]. Salivary glands produce 1 to 1.5 liters of saliva per day. Masticatory action has great influence on salivary output, being that, while it is happening and more fluid is being produced, thus, oral cleaning is promoted [44,45]. On the other hand, during the night, as the human body is resting, salivary flow rate is naturally

lower, which inevitably leads to an increase of microbial species in the oral cavity. As mentioned before, these species form micro-accumulations (biofilms) in implants gaps (between implant components) or between the gum/implant or gum/teeth interstices and secrete acidic metabolites, leading to a decrease on the salivary pH (around 5 – significantly lower than other places in the mouth), that combined with mechanical solicitations (caused, for instance, by normal chewing movements) might be harmful for the long-term performance of dental implanted systems [10,37]. It is clear that the saliva constitution, properties and flow are unique for everyone. It changes overtime as individuals grow, but also every day, as the conditions change [9].

The oral fluids pH consists in a critical factor for corrosion and tribocorrosion of dental implant materials. It can change quite rapidly due to external and/or internal factors. External factors like acids (e.g., lactic acid) and fluoride, introduced, respectively, by bacteria and teeth cleaning habits, as well as diet, tobacco consumption and the presence of microbial metabolites, can easily alter salivary pH and, thus, be determinant for the corrosion behavior of the dental implant [37,44]. Additionally, oxygen levels in the oral cavity are always changing, since variations can occur between the mucosal and sub-gingival areas, essentially when there is infection. Oxygen is almost absent in areas below the gingival margin so, consequently, microbial colonization occurs, which promotes the preferential growth of aerobic or anaerobic microorganisms. As oxygen is important for cathodic reactions during the electrochemical processes of metals, the corrosion kinetics can be affected [37]. As for internal factors, such as salivary gland dysfunctions and body temperature or, simply, the time of the day or the amount of stress the person is experiencing, they can strongly influence the oral environment [35,37].

Barão *et al.* [46] studied the influence of saliva pH on cp Ti and Ti-6Al-4V alloy corrosion behavior. For both materials, no significant differences were observed for the different pH values. At lower pH, Ti showed a decrease on the corrosion resistance due ionic transfer with saliva. The authors reported a significant increase on the corrosion rate, as Ti revealed a higher corrosion resistance than Ti-6Al-4V. Also, greater surface changes of Ti occurred at low pH values and, for the potentials and solutions used, no pitting corrosion was found.

Taking the saliva unstable nature into account, it is necessary to resort to AS solutions, to be able to test biomaterials *in vitro* to mimic the oral conditions. However, as saliva is constantly changing, these prepared solutions do not model many aspects of clinical conditions [37]. Organic-free artificial saliva solutions have been used in corrosion studies, and reviews about the composition and properties of many artificial saliva solutions, in the scope of dental implants corrosion behavior [47,48]. However, since Fusayama *et al.* [7] proposed modifications to a well-known synthetic saliva, already proposed by Meyer,

Fusayama´s artificial saliva (FAS) has been largely used as the electrolyte in studies about Ti corrosion behavior, since it is currently the closest to natural saliva [8,33,35,49–52]. In Table 3 is presented the composition of FAS.

Table 3 - Composition of the Fusayama's artificial saliva [33].

Compounds	**Concentrations (g/L)**
KCl	0.4
NaCl	0.4
$CaCl_2 \cdot 2H_2O$	0.795
$Na_2HPO_4 \cdot 2H_2O$	0.69
$Na_2S \cdot 9H_2O$	0.005
Urea	1

2.5.2 MASTICATORY FORCES AND STRESS DISTRIBUTION

Failure in dental implants has been attributed not only to biomechanical overloads but also to corrosion and wear synergy along with the cyclic loading mechanism of the masticatory process [37]. Human body features (age, gender, weight, muscle strength, whether they have, or not, dental implants, etc.) and food characteristics (hardness, ductility, size, thickness, Young´s modulus, etc.) dictate the intensity of mastication forces [10].

The mastication forces produced during the chewing cycle have been reported to be in the range of 10 to 120 N [52]. The highest mastication forces are generated at the end of the chewing cycle when sliding motion stops as the teeth reach the centric occlusion that produces localized abrasion wear of contacting dental surfaces [52]. According to Anusavice *et al.* [53] and Sevimay *et al.* [54], the maximum biting forces were measured by different methods, such as electromyography and occlusal transducers, and are in the range of 89 to 150 N at the incisors (anterior region), 133 to 334 N at the canines, 220 to 445 N at the premolars (intermediary region) and 400 to 600 N at the molars (posterior region).

Once the tooth is replaced, every dental implant should be able to support these forces, as the design and the material and its properties have a major role in the ability to withstand these forces. Besides the magnitude of the mastication forces, orientation is also a very important aspect to consider, since axial loads promote stress transfer through dental implanted systems to the bone tissue, and

oblique stresses can generate material and bone overload, which often leads to its failure by fatigue and wear [55–57]. Moreover, it is important to be aware of the fact that design aspects, such as shape, length and/or diameter, should be optimized in order to minimize stress distribution to the hard tissues, and, also, it is desirable that dental prostheses components are made out of rather similar materials, in order to have similar mechanical properties. Otherwise, abrupt variations may cause even more stress transportation to the maxilla or mandible bones [10].

During mastication forces, micro-movements can be found at the prosthesis interfaces: implant/crown, implant/abutment, implant/bone and abutment/crown. In these situations, fretting corrosion can happen, meaning that wear and corrosion occur simultaneously, in other words, synergistically [37]. In Figure 8 there are presented the loads an implant is subjected, as well as the location of possible micro-movements and gaps.

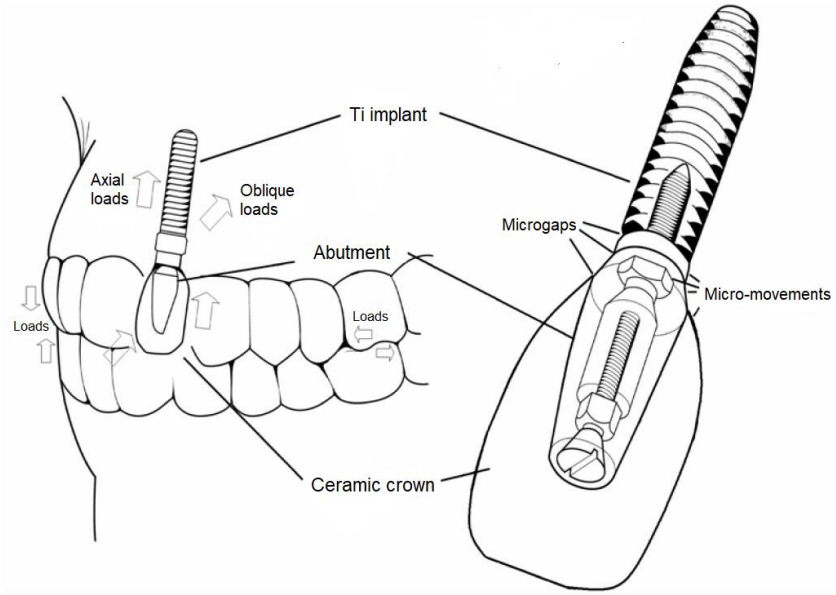

Figure 8 - Schematic representation of mastication forces and loads an implant is subjected. Adapted from [35].

2.6 CORROSION OF CP TI IN THE ORAL CAVITY

First and foremost, according to EFC, corrosion can be defined as "physicochemical interaction between a metal and its environment which results in changes in the properties of the metal and which may often lead to impairment of the function of the metal, the environment, or the technical system of which these form a part" [58]. Therefore, the term "corrosion" is referred as the process and the involved reactions, and not the outcome, frequently designated as corrosion damage or degradation.

Corrosion of metal implants is critical since it can adversely affect biocompatibility and mechanical integrity. Corrosion and surface film dissolution are two mechanisms for introducing

additional ions in the body. Extensive release of metal ions from the metallic structure can result in adverse biological reactions and can lead to mechanical failure of the device [27]. Ti has been a dominant topic of discussion for the past decades, in the dental implantology field, due to its attractive properties, regarding corrosion resistance and mechanical strength, and biocompatibility. A major reason for the large-scale use of Ti is due to its reported excellent corrosion resistance when inserted in the oral cavity [3].

Thus, in the scope of this thesis, corrosion behavior regarding cp Ti (Grade 2) used in endosseous implants was investigated. It is not only important to analyze this biomaterial when in contact with mimetic solutions of human saliva (such as FAS), but also to consider the presence and effect of certain additives (as a result of natural events, daily activities or surgical interventions) and the fact that the mouth is not a static environment. Saliva is a complex natural electrolyte that is constantly changing and, as a result, can interfere in the corrosion behavior of Ti. Besides its normal components, it might contain additional substances, such as fluorides, hydrogen peroxide (H_2O_2) and acids (citric acid, lactic acid, phosphoric acid) as a result of either bacteria and their metabolic activity or the ingestion of certain foods or drinks [33,34]. As aforementioned, the main goal of this this work was to understand the effects of the additives. Although the majority of these effects are still unknown to the science investigation community, they promote local changes of pH in the oral cavity, which can compromise the Ti efficiency.

Marino *et al.* [59] studied the electrochemical behavior of a dental screw made of cp Ti (Grade 2) in AS, during a period of 1500 minutes. EIS, OCP and potentiodynamic tests were performed and results evidenced the stability of the surface oxide layer that covers the implant, protecting it against corrosion up to 1.5 V at 25 °C, in AS. The resistance of the film decreased as the exposure time increased, due to the breakdown of the oxide layer followed by its dissolution. Chemical composition of Ti was analyzed and demonstrated that the maximum limits of interstitial elements (C, N, Fe and O) were altered, influencing its corrosion resistance.

2.6.1 INFLUENCE OF FLUORIDES

Corrosion induced by fluorides (F^-) is a problem since it is frequently found in oral health solutions for dental caries prevention such as toothpastes, gels and elixirs, as well as some drinking waters, and recently has been added in cooking salt [60]. Fluorides are used in oral hygiene solutions because they are able to suppress microbial growth and act as a buffer inhibiting bacterial acid production [61]. However, these products present pH levels of 3.5-7 and fluoride concentrations around 250 to 10.000

ppm, which means its continuous use may affect the corrosion, and tribocorrosion, behavior of dental implants [61–63].

Schiff *et al.* [62]performed some electrochemical tests using potentiometric and voltametric techniques, on cp Ti (grade 2) and some alloys in the presence of Fusayama-Meyer´s AS and certain concentrations of fluorides. The tests revealed interaction between the fluoride ions and Ti, which damaged the protective passive layer of the metal. The authors stated the importance to pay attention to the patients wearing titanium dental prosthesis should be advised not to use fluoridated products.

Moreover, high concentrations of F^- revealed localized corrosion, namely pitting corrosion, on Ti-based surfaces. The occurrence of this type of corrosion was reported to the formation of hydrated Ti oxides and salts, in the presence of hydrofluoric acid (HF) [51,64]. These investigations have proven that minimum concentration of 30 ppm HF is enough to promote a localized corrosion of titanium in fluoride solutions. Actually, corrosion in fluoride-rich solutions depends on the pH and the formation of HF produced by the dissociation of sodium fluoride (NaF), when present at high concentrations, or in low pH solutions due to the bonding between H^+ and F^- ions. As a result, localized corrosion on Ti surfaces might occur in a solution containing 452.5 ppm F^-, at pH 4.2, or in a solution containing 227 ppm F^- at pH 3.8. The formation of pits on cp Ti was also found in a previous study after immersing it in AS containing 11180 or 12300 ppm F^- [61,64]. Chemical analysis showed heterogenic oxides, such as $TiOF_2$ and $TiOHF$, were found in cp Ti, after immersing it at high F^-concentration [64].

2.6.2 INFLUENCE OF LACTIC ACID

Lactic acid (LA) ($C_3H_6O_3$) can also be found in the saliva as result of metabolic activity by bacteria [37]. Koike and Fujii [65–67] studies evidenced higher resistance to corrosion of Ti immersed in physiological saline and AS, and dissolution and discoloration when in contact with LA [65,66]. The authors also studied the corrosive properties of Ti in 128 mmol/L of lactic and formic acids at pH 1 to 8.5 for three weeks at 37°C. Results showed that the corrosive properties of titanium were markedly dependent on pH in formic acid and relatively less dependent on pH in LA. However, up to now, there have been few reports studying the effect of LA amount, and the mechanism remains unclear [67]. On the other hand, Qu *et al.* [68] investigated the corrosion behavior of pure titanium in AS and concluded that the addition of lactic acid into AS solutions can distinctly accelerate the corrosion rate, and the corrosion of titanium is aggravated with increasing the amount LA. Additionally, SEM images indicated that LA can accelerate the pitting corrosion in AS.

2.6.3 INFLUENCE OF HYDROGEN PEROXIDE

As lactic acid, hydrogen peroxide (H_2O_2) is an important oxidizing compound produced by bacteria and leukocytes, which are freed into the oral cavity during an inflammation process, as a consequence of surgical trauma or abscesses [60]. Moreover, H_2O_2 is able to damage microbial cell walls, however, at the same time, it is not able to recognize the cells is in contact and, therefore, differentiate which ones are the host´s and the attacker´s. This way, H_2O_2 can be detrimental to biomaterials since it compromises cell viability and, thus, osseointegration of the implant [37]. Actually, H_2O_2 has proven to have a damaging effect on Ti. Mabilleau *et al.* [60] investigated the corrosion resistance of cp Ti disks for nine days of immersion in different media: AS containing F^- (at concentrations 0.5 % and 2.5 %), H_2O_2 (at concentrations 0.1 % and 10 %) and/or LA. It was demonstrated that the combined action of these additives resulted in a considerable increase of Ti corrosion, as well as intensifying its surface roughness, which may influence the tribocorrosion behavior.

2.6.4 INFLUENCE OF CITRIC ACID

Ascorbic (also commonly known as vitamin C) and citric acids ($C_6H_8O_7 \cdot H_2O$) can be detected in the mouth due to food breakdown. The citric acids are commonly found in many fruits, vegetables, or drinks. Vieira *et al.* [34] combined citric acid with AS and proved it enhances the oral environment corrosivity, however, contrariwise, it appears to provide a protective effect to Ti under fretting corrosion conditions. Kedici *et al.* [69] verified that Ti demonstrated high corrosion resistance in FAS with citric acid, while with other alloys whose behavior was being investigated as well must be carefully examined.

2.6.5 INFLUENCE OF PHOSPHORIC ACID

Phosphoric acid (PA) (H_3PO_4) is another additive to consider, as it is often found in some foods, especially dairy products such as milk or cheese. Ghoneim *et.al* [70] studied the influence of PA concentration and temperature on pure Ti and Ti-6Al-4V alloy electrochemical behavior was investigated using OCP and EIS tests, over a range of acid concentration (1 to 14 M), where lower concentration of PA lead to lower corrosion susceptibility (from OCP) and higher corrosion resistance (from EIS) than higher concentration of PA. In OCP measurements was registered initial positive shift in potential associated with thickening of the oxide film formed on the material surface. Moreover, as the concentration of PA increased, potential changes towards more negative values are shown due to the

thinning and dissolution of the film. The EIS tests confirmed this trend, since the corrosion current density values, at any given temperature, were higher for the alloy as compared to those for the metal. Also, at any given temperature, Ti oxide film showed higher thickening rate, in 1 M PA medium.

2.7 ELECTROCHEMICAL TECHNIQUES FOR CORROSION BEHAVIOR ANALYSIS

In literature, there are many electrochemical techniques to investigate the corrosion behavior.

OCP is one of them and its results provide information about the electrochemical state of a material, showing if the material is on an active or passive state. In other words, it is useful to examine the corrosion susceptibility. However, there is important information this technique is not able to give, specifically, concerning corrosion kinetics [71].

PDP is another useful technique since it provides information about electrochemical reactions kinetics, through measurement of current density values while changing the applied potentials to the metallic samples [71].

Furthermore, EIS is an even more complete technique, as it nondestructive and provides a detailed analysis of electrochemical reactions, mechanisms and kinetics. After the stabilizing the system (achieved in OCP), it gives information about the properties of the passive film and localized corrosion mechanisms, and it allows the study of species adsorbed on the materials surface [71].

2.8 TRIBOCORROSION OF CP TI IN THE ORAL ENVIRONMENT

In dental implantology, both electrochemical and mechanical solicitations are determinant to the implant clinical performance and success. The ASTM standards succinctly define tribocorrosion as *"a form of solid surface alteration that involves the joint action of relatively moving mechanical contact with chemical reaction in which the result may be different in effect than either process acting separately"* [72]. Also, according to Mischler *et al.* [73] and Landolt *et al.* [74], tribocorrosion consists in the irreversible degradation phenomena of a material caused by simultaneous mechanical (wear) and electrochemical (corrosion) actions on surfaces subjected to a relative tribological contact movement, in a corrosive medium. In this sense, a tribocorrosion system is complex to understand since both transformation mechanisms affect each other mutually [75].

It is reported that passive metals such as Ti are particularly sensitive to tribocorrosion phenomena, since sliding can destroy the passive film, leading to the increase of both corrosion and wear rates, before the surface repassivation [76,77].

2.8.1 TRIBOCORROSION: SYNERGISM BETWEEN CORROSION AND WEAR

Corrosion is a major cause of Ti implants degradation due to the corrosive nature of the oral environment (saliva and its additives). However, as these structures are implanted in the mouth they are also subjected to mechanical actions such as masticatory forces or sliding and fretting (cyclic micromovements) at implant/crown, implant/abutment, implant/bone interfaces. This constitutes a tribocorrosion system. The combined action of corrosion and wear lead to the increased release of metallic ions and wear debris, which cause toxicity and, therefore, compromise, the material biocompatibility [37,78].

In a tribocorrosion system, a synergism between mechanical and chemical actions of environmental effects is observed, which can have negative consequences depending on the properties and characteristics of the materials surface and reaction products, as well as on the composition of the local environment. A corrosive environment can amplify the rate of material loss by wear mechanisms, while wear can increase the corrosion rate by damaging and detaching the protective TiO_2 passive film [10,79,80].

In Figure 9 is presented a schematic representation of the different tribocorrosion mechanisms of titanium while rubbing against a hard counter-body made of alumina, which is often used in dental crowns [10,81]. As the rubbing motion begins, localized disruption of the protective layer may occur, exposing the bulk metal to the oral environment. This leads to the formation of micrometric oxide third-body particles (wear debris), which play a critical role as they can have negative effects, when they are abrasive, and therefore, accelerate mechanical wear, or positive effects when they act as a solid lubricant and mitigate friction, and consequently, wear [81]. As this happens, the metallic surface tries to reinstall its protective film (repassivation), leading to an increase of the metal internal energy due to severe plastic deformation, which will compromise the corrosion behavior of Ti [74].

The wear products can be transferred and deposited on the alumina surface or spreaded on the Ti surface forming oxide tribolayers. When abrasive, these layers can aggravate the wear mechanisms and, on the other hand, as it all takes place in an electrochemical environment (oral cavity), dissolution may happen, exposing fresher and more reactive metal. In this way, a galvanic cell is established and the corrosion rate is drastically increased. As a result of these two mechanisms involved in a tribocorrosion system, metallic debris and ions are released to the surrounding tissues, which can cause inflammatory reactions and incompatibility [37,74]. Thus, it is vital to minutely investigate the tribocorrosion mechanisms and effects in severe conditions, so that the implant does not fail when implanted in the mouth [37].

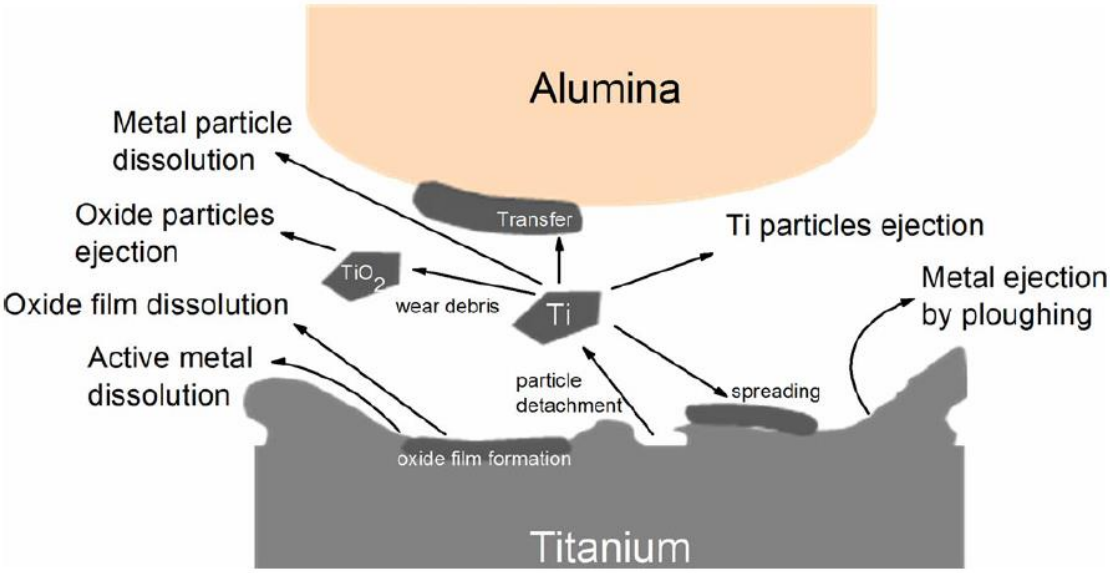

Figure 9 - Schematic representation the different tribocorrosion mechanisms of titanium while rubbing against alumina [10].

2.8.2 TRIBOCORROSION SET-UP

The synergism between corrosion and wear is a complex system so, in order to study it, corrosion and wear have to be monitored simultaneously. To perform tribocorrosion tests, it is important to know the possible tribological contacts, as well as test set-up (tribometer), in order to understand the synergistic effects.

2.8.2.1 TRIBOLOGICAL CONTACTS

Wear can be defined as the progressive loss of material resulting from mechanical interaction occurring between two contacting surfaces, which are in relative motion, and under load [82].

Wear and its debris are critical factors on the implant lifetime and biofunctionality, especially when allied to a corrosive environment. In order to study the wear contribution on tribocorrosion mechanisms of dental implants, it is crucial to know the possible tribological contacts. According to Landolt *et al.* [74], materials degradation due to simultaneous chemical and mechanical effects may occur under a few possible tribological contacts, such as sliding (unidirectional or reciprocating), fretting, rolling or impingement, as shown in Figure 10.

Sliding contacts can occur as a two body or three body system (resultant of the rubbing motion), and the relative motion can be unidirectional, as in a pin-on-disk wear test, or reciprocating/bidirectional, as in a pin-on-plate test apparatus [74].

Fretting is considered a special type of sliding contact because it consists on cyclic stresses, which can also happen in two body or three body arrangements. In other words, it is a form of reciprocating sliding, but with small amplitude motions (micromovements) [74]. According to Kumar *et al.* [83], fretting corrosion is a major factor on the Ti implants clinical failure, under *in vivo* conditions. Fretting corrosion of Ti and its alloys has been studied in simulated body fluids, where the synergism between wear and corrosion seems to increase metal degradation [78].

In rolling conditions, a cylinder or sphere rolls against a smooth surface, causing friction. And finally, impingement is a consequence of the impact of particles on a smooth surface. If the motion is perpendicular to the surface, impingement attack is observed, and if it is parallel, there is surface erosion [74].

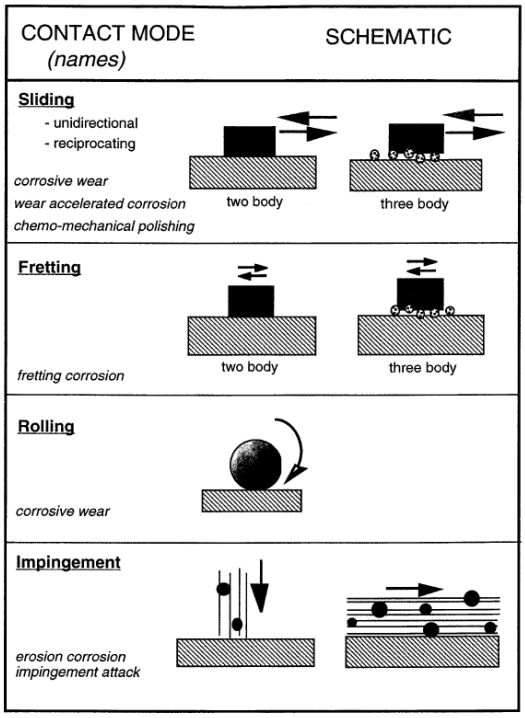

Figure 10 - Schematic representation of the different types of tribological contacts involving simultaneous mechanical and chemical effects [74].

2.8.2.2 TRIBOCORROSION ARRANGEMENTS

In the tribological contacts aforementioned concerning tribocorrosion systems, different types of arrangements involving an antagonist (or counter-body) rubbing against a flat plate can be used. The counter-body can be a cylindrical pin, a truncated cone, or a sphere, as seen in Figure 11. Unlike spherical contacts, a flat pin surface as the cylindrical is not free from alignment problems and has a well-defined nominal contact area, which is an advantage [80].

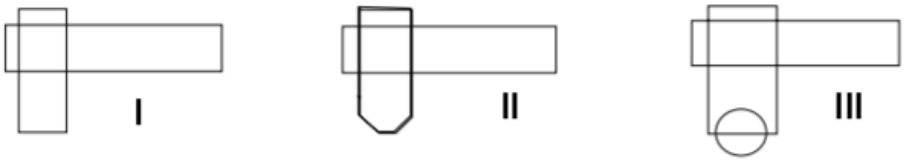

Figure 11 - Types of counter-body: (I) cylindrical pin, (II) truncated cone and (III) sphere. Adapted from [74].

In order to have a tribocorrosion system, an electrolyte solution is required. The conventional pin-on-disk arrangement that includes an immersed stationary disk (or plate) rubbing against an oriented rotating spherical pin are not well suited for being immersed in an electrolyte (Figure 12 (a)). In Figure 12 (b) is represented pin-on-plate apparatus, which consists in a pin sliding in linear reciprocating motion on an immersed stationary plate. The arrangement presented in Figure 12 (c) includes a downwards rotating disk contacting with a stationary pin, while the electrolyte solution is ejected through below nozzles. However, this can also be used with in an immersed contact, rather than the nozzles. Lastly, in Figure 12 (d), a ceramic microtube, included in a second tube containing the electrolyte, rotates on a stationary metal plate, allowing measurements of the tribocorrosion behavior locally on very small surfaces, sacrificing the fidelity of mechanical control [80].

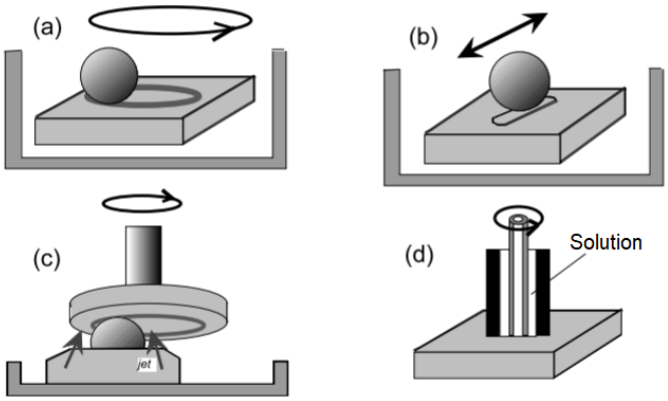

Figure 12 - Experimental arrangements used in tribocorrosion studies: (a) pin rotating on immersed plate, (b) reciprocating motion of pin on immersed plate, (c) stationary sphere on rotating disk with electrolyte injection from below, (d), rotating ceramic microtube serving as electrolyte conduit. Adapted from [74].

The results obtained by Landolt *et al.* [80] indicated similar coefficient of friction values when different tribocorrosion arrangements were used. On the other hand, significant differences were observed in the wear volume quantification, as well as in the current density measurements.

2.8.2.3 TRIBOCORROSION EQUIPMENT AND ELECTROCHEMICAL TECHNIQUES FOR *IN VITRO* STUDY OF TRIBOCORROSION

In order to investigate *in vitro* tribocorrosion on dental implants, in mimic conditions of the oral environment, and study the synergistic action of corrosion and wear, both have to be monitored simultaneously with special equipment. Barril *et al.* [78] developed a novel apparatus (such as the one showed in Figure 13 to study the fretting–corrosion behavior of metallic materials used in prosthetic implants that combines a precise control of mechanical and electrochemical variables, and the data showed good reproducibility of the measurements.

In Figure 13 is showed a tribocorrosion set-up, which consists in a potentiostat is coupled to a tribometer, where an electrochemical cell with a reference electrode (RE), working electrode (WE), which is the sample, and, when necessary, a counter electrode (CE), in order to get data on electrochemical and tribological mechanisms simultaneously.

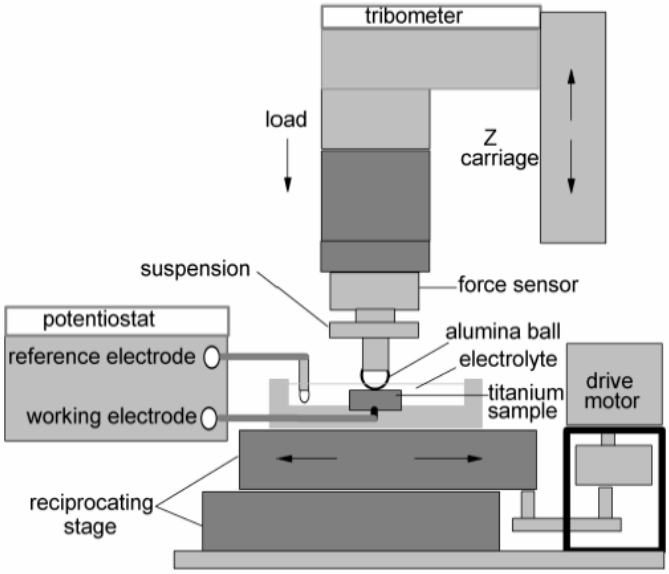

Figure 13 - Schematic representation of a tribocorrosion set-up [79].

Ponthiaux *et al.* [71] pointed electrochemical techniques, such as OCP, PDP and EIS to investigate combined corrosion and wear degradation of materials in sliding contacts immersed in electrically conductive solutions. Performing these techniques assembled to a tribological test provide crucial and meaningful data to understand tribocorrosion parameters (such as the electrochemical reactions nature, existence of protective passive films, interactions between electrochemical reactions and friction) and the kinetics of corrosive reactions (such as corrosion rate, depassivation rate by mechanical action in the contact area and film passivation rate). Besides, electrochemical measurements can give information on the tribological conditions of friction and wear mechanisms, as sliding friction,

the electrochemical state of the surfaces is highly influential on the wear process in the contact region, showing signs of mild oxidation, abrasive wear, among others.

Furthermore, Mischler [84] published a critical paper on the main electrochemical methods used in tribocorrosion research with special emphasis on sliding and fretting situations involving passive metals. It was reported that, for tribocorrosion studies, OCP and PDP are the most used techniques.

OCP results are determined by surface factors, such as the ratio of worn and unworn surfaces, being the worn where the fresh metal is exposed to the electrolyte due to protective film removal and unworn are where the passive film is intact. Moreover, the repassivation kinetics of the bare material in exposed regions, the contact frequency and load [71,84]. As an example, Figure 14 a) is represented an OCP test schematic set-up, under rubbing conditions, with an alumina ball as the counter-body, where the corrosion potential (E_{corr} or OCP) of an immersed (0.9% NaCl solution) Ti-6Al-4V sample is being monitored with a potentiostat. The results in Figure 14 b) show that, as the rubbing begins, the E_{corr} of the material shifts to lower values, also known as cathodic shift. During sliding, the measured corrosion potential reflects the two surface states, with the passive metal (unworn area) and the fresh metal (worn area) exposed to the electrolyte, as reported by Ponthiaux *et al.* [71]. In this case, the oscillations on E_{corr} due to represent the material's attempts of passivating the worn areas by the ceramic ball. As the rubbing motion stops, E_{corr} is able to reach the similar values as the initial ones due to repassivation mechanisms, as the Ti alloy fully recovers its protective surface layer.

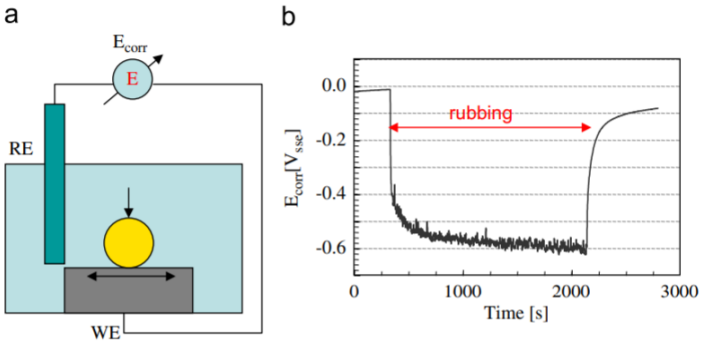

Figure 14 - (a) Schematic representation of a tribocorrosion test set-up with the measurement of the E_{corr} (RE: standard silver chloride electrode, SCE) and (b) evolution of the E_{corr} of a Ti-6Al-4V alloy rubbing against an alumina ball in 0.9% NaCl solution [84].

In Figure 15 a) is presented a schematic potentiostatic test set-up, where a selected anodic potential is imposed to an immersed (0.9% NaCl solution) Ti-6Al-4V sample, using a three-electrode (WE, RE and CE) set-up connected to a potentiostat. In this case, current density values are measured as a function of the time to assess electrochemical reactions kinetics, in tribocorrosive conditions. Important to note that

this experiment is performed after the stabilization of the OCP. As the rubbing begins, an abrupt increase in current density occurs due to oxidation reactions of the fresh metal exposed to the electrolyte, after abrasion of the passive film on its surface. During sliding motion of the ceramic ball, current density values suffer little oscillations due to the surface's galvanic coupling of worn and unworn areas, as it tries to reinstate the passive film. When rubbing stops, current density decreases to a similar value of the one before the mechanical solicitation because the Ti alloy sample is fully repassivated [84].

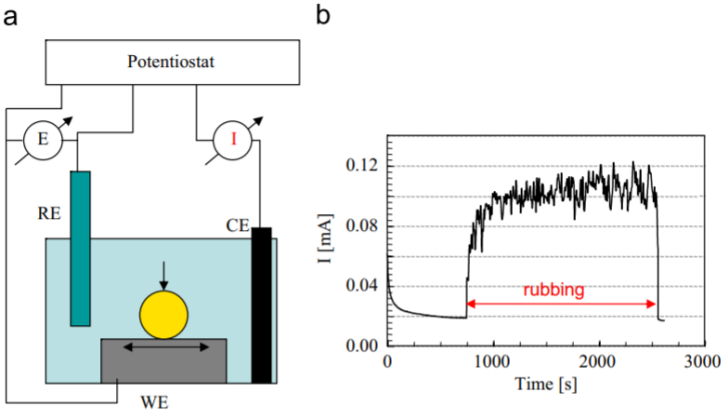

Figure 15 - (a) Schematic view of a tribocorrosion experimental set-up including a potentiostatic set-up and (b) evolution of the current density values of a Ti-6Al-4V alloy rubbing against an alumina ball in 0.9% NaCl solution at imposed potential of 0.3V_{SCE} (RE: standard silver chloride electrode, SCE) [84].

On the other hand, performing PDP tests can be profitable since they provide detailed information on electrochemical reactions kinetics alterations due to sliding, and allow to understand the influence of surface reactions on sliding conditions in the contact region. Mechanical depassivation rate of worn surfaces, corrosive wear rate and the mechanism of mechanical wear are other parameters which PDP when used in a tribocorrosion system [71]. Finally, with EIS it is possible to understand, in detail, the electrochemical reactions kinetics, under sliding contacts, and the interaction between friction and corrosion. In these last techniques, results can be to interpret due to the surfaces topography and chemistry heterogeneity [71,84].

2.8.3 FACTORS THAT AFFECT TRIBOCORROSION IN DENTAL IMPLANTS

Tribocorrosion behavior is a complex system, as it is highly dependent on the properties and characteristics of the contacting materials, the mechanical aspects of the tribological contact and the properties of the surrounding environment, as shown in the scheme displayed in Figure 16 [38,78]. These parameters are combined in a synergistic or antagonistic way, which can be favorable or not for the tribocorrosion system [80].

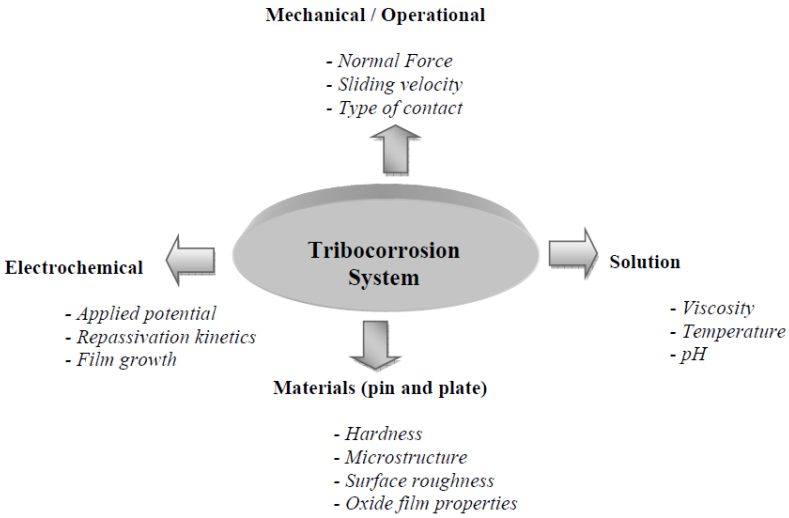

Figure 16 - Schematic representation of the parameters that influence a tribocorrosion system [38].

Regarding mechanical aspects, the tribocorrosion rate for a certain metal-environment combination depends on distribution and frequency of application of load and contact pressure, contact geometry and type - sliding, fretting, rolling or impingement. It is important to note that frequency and velocity are critical parameters once that they determine the depassivation rate [80].

In dental implants, masticatory forces will endorse, as well as amplify, the development of cyclic micro-movements at implant/bone or implant/abutment or implant/ceramic crown interfaces. The type of movement may be fretting or reciprocating sliding, depending on its amplitude and frequency [13].

In a tribocorrosion system, the parameters, such as hardness, topography, morphology, chemical composition, microstructure and the presence or not of an oxide film (and its properties), of the participant materials in the tribological contact are crucial [80].

Lastly, dental implants are placed in the oral cavity, so, naturally, it is going to interact with the saliva and/or body fluids. Its chemical composition, pH, temperature, the presence of additives, and, sometimes, consequent formation of biofilms are prime factors to take into consideration [80].

2.8.4 TRIBOCORROSION STUDIES OF CP TI FOR DENTAL APPLICATIONS

Recently, the need for more information regarding tribocorrosion behavior of metals such as cp Ti, regarding dental applications is growing in order to understand the corrosion-wear mechanisms and how the oral environment affects the materials corrosion-wear mechanism.

Mathew *et al.* [85] performed unidirectional sliding tests to cp Ti disks, with a ceramic ball, in FAS at three different pH values (3, 6 and 9). EIS measurements performed before and after sliding showed that, after sliding, the corrosion resistance increased probably due to the coupled action between

the characteristics (higher corrosion resistance) of the passive film formed in the unworn area and the chemical reaction in the worn area. On the other hand, a worse tribocorrosion behavior as observed at pH 6.0 evidenced by the highest weight lost and greater tribocorrosion damage proved by the cracks observed on the SEM images. Despite reports of cp Ti being electrochemically stable down to pH 2.0, this study suggests degradation peaks at near neutral pH values when mechanical solicitations are involved.

The influence of fluorides (F^-) on the tribocorrosion behavior of cp Ti (grade 2) in FAS was studied by Souza *et al.* [33] under reciprocating sliding. F^- content ranged from 20 to 12 300 ppm, leading to a pH variation from 5.5 to 6.5. Tests were conducted at room temperature and the OCP monitored. In solutions free of or containing low F^- concentrations (up to 227 ppm), cp Ti was able to establish a compact passive film. EIS tests showed the corrosion resistance of cp Ti decreased as F^- concentration increased. The coefficient of friction and subsequent wear, in FAS at low F^- (227 ppm) concentrations, is quite similar. On the other hand, for higher F^- concentration (12 300 ppm), the OCP presented almost negligible variations during sliding, since it is impossible to form the passive film in those conditions. Also, coefficient of friction recorded on titanium revealed a substantial decrease attributed to the presence of reaction product layers, and an increase of material loss was noticed. Thus, F^- amplifies the environments harshness and promotes the destruction of the Ti oxide film, which may lead to implants failure. Also, the wide spreading of wear debris close to the surrounding may induce peri-implant inflammations and toxic effects to the human body.

Vieira *et al.* [34] investigated the tribocorrosion behavior of cp Ti in FAS without (pH 5.5) and with citric acid (pH 3.8), in fretting conditions. The authors stated that the acidic saliva (with citric acid) had a protective-like role, as it slightly improved the tribocorrosion behavior of Ti. This behavior was attributed to the nature of oxidation and reduction reactions in the contact area. Despite no significant differences in the wear rate in function of the dissipated energy, in those conditions, it showed lower wear volume, which is linked to the slightly lower corrosion rate of the citric acid solution, during the fretting tests. Also, tribolayers were formed in the contact area during the tribocorrosion test, which are more stable when reached, approximately, 7000 cycles in FAS containing citric acid, as confirmed by the lower coefficient of friction and corrosion current.

When tribocorrosion occurs in the oral environment the presence and accumulation of microorganisms and its metabolites bring further complexity in understanding the material deterioration mechanisms generated by the synergic action of wear and corrosion. In fact, the interaction of metallic

surfaces with tribocorrosion products, bacteria, and their metabolic products may increase corrosion damage, as a result of the dissolution of metallic ions in the human body [37,86].

Souza *et al.* [87] performed tribocorrosion tests on cp Ti (grade 2) samples covered mixed biofilms of *S. mutans* (lactic acid- producing bacteria) and *C. albicans* (found in peri-implant sites), immersed in FAS (pH 5.5), with reciprocating sliding conditions against an alumina ball. Biofilms lead to a decrease on the pH down to 4, due to the secretion of acidic substances. At low normal loads of 100 mN, biofilms significantly reduced friction on cp Ti during sliding. On the other hand, EIS results showed that the reduction of the corrosion resistance of the metal, which is attributed to the acidic environment. Also, OCP measurements were also lower, which means the corrosion susceptibility increased in acidic conditions. However, these biofilms were removed when the applied normal load was 200mN. In both cases, when the friction is reduced and the fresh metal is exposed to the corrosion-wear interactions, mechanical integrity of the metal may be disrupted, causing the failure of the implant. Since most accumulations of microorganisms and acidic substances can be found microgaps on dental implants, it is crucial to avoid these gaps by designing optimized dental structures less susceptible to localized corrosion.

After an intense research on the effect of the most relevant additives on the corrosion and tribocorrosion behavior of cp Ti, there are not studies that approach it all, especially in terms of tribocorrosion, which is ultimately reflects what the oral cavity is: a tribocorrosion system. So, in order to get the best and most complete knowledge in terms of how this material interacts and reacts with the surrounding environment when implanted, *in vitro* analysis with parameters that mimic the condition changes in the mouth is crucial.

3 MATERIALS AND METHODS

3.1 CP TI SAMPLES PREPARATION

Cp Ti (Grade 2) plates (20x20x2 mm) were ground down to #600 mesh SiC paper. After, the samples were cleaned in ultrasound with propanol, for 5 minutes.

To ensure equal conditions for all samples, by removing all impurities, grinding marks and destroying any passive film previously formed, followed by the growth of a new oxide film, under controlled conditions, the samples were etched with a Kroll reagent (V_{HF}:V_{HNO3}:V_{H20} = 1:1:1) during 30 s. After that, the Ti samples were cleaned in an ultrasonic bath with propanol for 10 minutes and distilled water for 5 minutes, and lastly dried with hot hair.

3.2 ELECTROLYTE PREPARATION

As an electrolyte and a base for other electrolytes to be used the electrochemical and tribo-electrochemical tests of the control group, Fusayama's artificial saliva (FAS) [60,64,88] was prepared with a pH of 5.50 ± 0.25. In Table 4 is included information related to the FAS constituents, apart from distilled water.

In order to study the influence of lactic acid ($C_3H_6O_3$, LA), solutions of 2.5 g/L (pH 2.40 ± 0.33) and 5 g/L (pH 1.91 ± 0.02) were prepared with FAS. The LA used is from the brand Riedel-de Haën, with 88-92% purity. Solutions of FAS with phosphoric acid (H_3PO_4, PA) were also prepared with 1 M (pH 0.75 ± 0.45) and 14 M (not possible to measure the pH due to the solutions high acidity). The PA used is from Honeywell brand, with 85% purity. The pH values were measured with CyberScan pH 510 from Eutech Instruments.

Table 4 - Constituents of FAS and their brand, purity and concentration to use [33].

Constituent	Brand	Purity (%)	Concentration (g/L)
NaCl	Panreac	99.5	0.4
KCl	Panreac	99.5-100.5	0.4
$CaCl_2 \cdot 2H_2O$	Riedel-de Haën	≥ 99	0.795
$Na_2HPO_4 \cdot 2H_2O$	Riedel-de Haën	≥ 99	0.005
$Na_2S \cdot 9H_2O$	Sigma-Aldrich	≥ 98	0.69

3.3 ELECTROCHEMICAL TESTS

Electrochemical tests consisted in open-circuit potential (OCP), electrochemical impedance spectroscopy (EIS) and potentiodynamic polarization (PDP), using a three-electrode setup, at body temperature (37 °C) with 200 mL of electrolyte. The cp Ti plates, with an exposed area of 0.38 cm^2 to the electrolyte, were established as the WE. A platinum (Pt) wire mesh was used as the counter electrode (CE) and a saturated Ag/AgCl electrode as the reference electrode (RE).

Electrochemical tests were carried out with a Reference 600+ potentiostat/galvanostat/ZRA from Gamry Instruments. OCP was monitored for 3 hours in order to evaluate the corrosion potential of cp Ti when contacting with each electrolyte, as well as to stabilize the system, which was considered stable as long as the OCP values did not present higher variation than 60 mV in the last hour of the immersion. Since OCP monitorization gives information only on the susceptibility to corrosion, other techniques, such as EIS and PDP were performed in order to have a better understanding on the corrosion resistance and corrosion rate. The EIS diagrams were obtained at the OCP, by applying a 10 mV sinusoidal potential through a frequency range of 1 MHz to 10 mHz. Lastly, PDP measurements were recorded from –0.25 V_{OCP} to 1.50 $V_{Ag/AgCl}$ using a scanning rate of 0.50 mV/s.

To note that, at least three samples were studied for each electrolyte in order to assure reproducibility and all the electrochemical results are presented as average ± standard deviation.

3.4 TRIBO-ELECTROCHEMICAL TESTS

In order to perform tribo-electrochemical tests at OCP, cp Ti samples were placed and fixed in a tribo-electrochemical cell and immersed in 30 mL of electrolyte at body temperature (37°C). The cell was installed in the tribometer with a reciprocating ball-on-disk apparatus (Bruker CETR-UMT-2), where a 10 mm of diameter alumina ball (Ceratec) was used as counter-body. Tribo-electrochemical measurements were obtained via a two-electrode configuration (Ag/AgCl as RE and cp Ti samples as WE) coupled with a Reference 600 potentiostat/galvanostat/ZRA from Gamry Instruments.

Before sliding, as in the electrochemical tests, OCP was monitored for 3 hours, in order to stabilize the system, which was considered stable as long as the $\Delta E<60$ mV/h. The OCP was monitored before, during and after sliding. The sliding time was set as 30 minutes. During sliding, the coefficient of friction (COF) values were also measured during sliding. All tests were performed with 3 mm amplitude, frequency of 1 Hz and normal load of 1 N. For all groups, at least three tests were performed in order to assure the repeatability of the results. After each test, the samples were rinsed with distilled water.

For the potentiostatic tests, the samples were prepared the same way as OCP tests using the tribo-electrochemical cells. On the other hand, after fixing the tribo-electrochemical cell to the tribometer, a three-electrode configuration was used, with Ag/AgCl as RE, Pt wire mesh as CE and cp Ti samples as WE (exposed area of (2.6 ± 0.4) cm^2), coupled with a Reference 600 potentiostat/galvanostat/ZRA from Gamry Instruments. As a counter-body, a 10 mm of diameter alumina ball was used in order to have a reciprocating ball-on-disk apparatus.

These tests were carried out in two steps. First, before sliding, the OCP values were monitored for 5 minutes. Then, for 50 minutes, a constant anodic potential of +0.5 $V_{Ag/AgCl}$ was applied to the samples while the current density evolution was monitored before, during and after sliding. During the first 10 minutes, the current density stabilizes, and then, waited 150 seconds, the sliding started, lasting 30 minutes. The remaining time was used for the material recovery. All the tests were performed with 3 mm amplitude, frequency of 1 Hz and normal load of 1 N. For all groups, at least three tests were performed in order to assure the reproducibility of the results.

After removing the electrolyte, the wear products were collected for characterization. Lastly, the samples were rinsed with distilled water.

3.5 CHARACTERIZATION

After the tribocorrosion tests, an optical microscope (Leica-DM2500, Germany) and SEM/EDS (FEI QUANTA 250 FEG-SEM/Oxford Aztec EDX) with backscattered (BSE) and secondary electron (SE) configuration were used to characterize the wear tracks and wear products. The wear volumes, profiles and roughness were obtained by using a non-contact 3D profilometry (Profilm3D). Vickers hardness (HV) (EMCO-TEST DuraScan) was also measured in eleven points, inside and outside the wear tracks, of the samples with a 0.5 kg normal load.

4 RESULTS AND DISCUSSION

To ensure equal conditions for all surfaces, the cp Ti surfaces were etched in Kroll's reagent so that any previously formed passive film will be removed together with any impurities and grinding marks, leading to the growth of a new oxide film, under controlled conditions. Figure 17 shows the morphology of the cp Ti surfaces after etching, where can be observed the typical granular structure of Ti, that will be the benchmark for the following discussions. Same procedure was performed by Sousa *et al.* and Costa *et al.* [89,90].

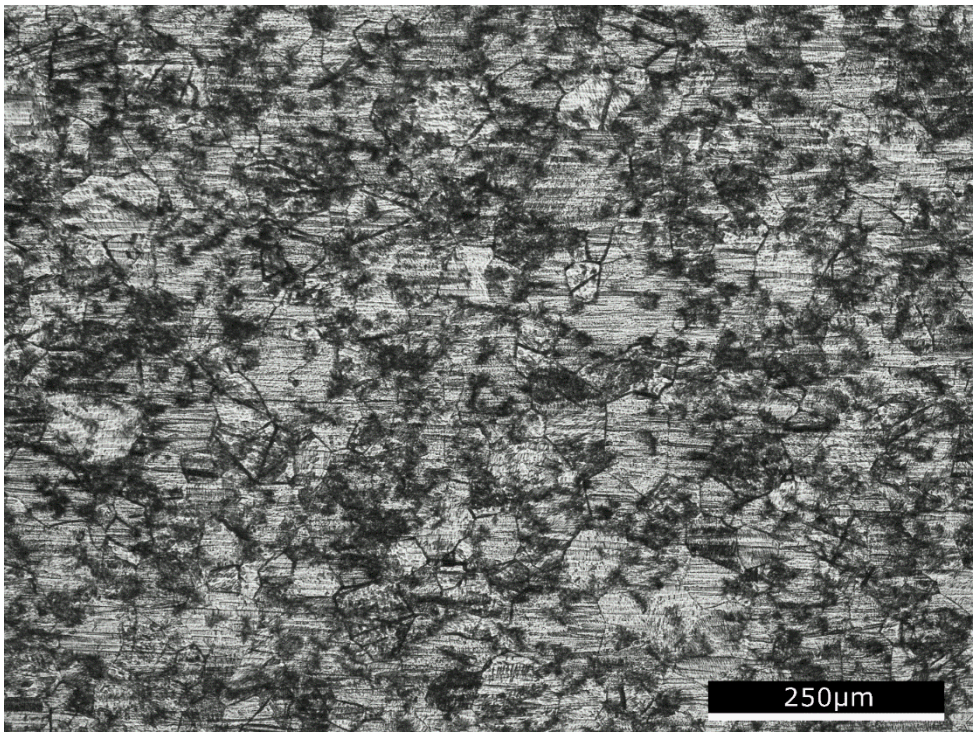

Figure 17 - OM image of a cp Ti surface after etching.

4.1 ELECTROCHEMICAL BEHAVIOR

Before performing EIS and PDP, the OCP was performed in order to stabilize the system, through the formation of a passive film. In Figure 18 a) are shown the E_{OCP} for the cp Ti samples immersed in the different proposed solutions, for the last 5 minutes of immersion. In Table 5 are presented the average E_{OCP} values.

When immersed in non-additivated AS, cp Ti presents an E_{OCP} of (−0.309 ± 0.039) $V_{Ag/AgCl}$. By adding lactic acid (LA) in 2.5 g/L or 5 g/L, E_{OCP} is increased, meaning that cp Ti tendency to corrosion decreases. Nevertheless, when comparing the effects for both concentrations, when the lowest concentration of LA was added led to a slightly lower corrosion susceptibility. This tendency is congruent with Qu *et al.* [68] study on the influence of the amount of LA to artificial saliva on the corrosion behavior of titanium, at 37°C. The authors reported that E_{OCP} increased with increasing concentration of LA from 0 to 3.2 g/L, due to the growing adsorption to the metallic surface. However, from 3.2 g/L LA upwards, OCP started to slightly decrease as the maximum level of adsorption is reached and it starts to separate from the surface.

In the case of phosphoric acid (PA), when added in a lower concentration (1M), it did not have a significant effect on the corrosion susceptibility of cp Ti, since the E_{OCP} values are similar to the AS. On the other hand, when PA 14M is added to AS, the tendency to corrosion is significantly worsened. Ghoneim *et al.* [70] studied the effect of PA concentration in triply distilled water on cp Ti corrosion, at 298 °K (approximately, 25 °C), and reported similar results, since the E_{OCP} became more positive, until stabilizing, across PA 1M, 3M and 4M, which is directly related to the thickening of the passive film. On the other hand, from PA 6M upwards, it was reported a negative shifting of the OCP for PA 10M and 14M due to the active dissolution before stabilization. Thus, PA 14M provided the lowest E_{OCP} after 90 minutes of immersion.

Representative potentiodynamic polarization curves are presented in Figure 18 b), along with the extrapolated corrosion potential ($E_{(i=0)}$) and passivation current density (i_{pass}) values, together with E_{OCP}, that are presented in Table 5. In the cathodic region, below $E_{(i=0)}$, cathodic reactions prevail, and corrosion of cp Ti is inhibited. As soon as anodic and cathodic reactions rates are the same, when $E_{(i=0)}$ is reached, the anodic domain is started. Initially, there is an active region, where there is an increase in the current density values, which is directly related to an increase in cp Ti corrosion rate. When in contact with AS, AS+LA or AS+PA 1M, cp Ti presents its typical curve, meaning that, from $E_{(i=0)}$ upwards, the increasing current density ends when i_{pass} is reached, followed by a well-defined passivation plateau, indicating the passivation of the metal. This typical behavior of cp Ti is well reported in the literature [64,89,91,92] .

In a more detailed analysis, despite the lower corrosion susceptibility attributed to higher $E_{(i=0)}$, the addition of LA to AS, in both concentrations, resulted in slightly the same corrosion behavior for cp Ti, due to the relatively close i_{pass} values. Nonetheless, the recorded i_{pass} evidenced higher corrosion rate as LA is added to AS. Moreover, for AS, AS+ LA 2.5 g/L and AS+LA 5 g/L, i_{pass} is reached at (0.025 ± 0.064) $V_{Ag/AgCl}$, (0.136 ± 0.058) $V_{Ag/AgCl}$, (0.234 ± 0.149) $V_{Ag/AgCl}$, respectively. This may indicate that, as LA concentration increases, cp Ti reaches its passive state for higher applied potentials, suggesting, once again, its lower corrosion susceptibility. Qu *et al.* [68] also performed potentiodynamic polarization tests on cp Ti and the results showed that, although, visually, the differences between LA concentration curves appeared to be negligible, when analyzing the polarization parameters, $E_{(i=0)}$ was less negative as LA concentration increased from 2.5 to 5 g/L, being that non-additivated AS resulted in the lowest values, regardless of the immersion time, confirming the lower tendency to corrosion without LA. Nonetheless, i_{corr}, which translates corrosion rate, increased with the amount of LA, meaning that increasingly high LA concentration, indeed, accelerates corrosion of cp Ti, more significantly for higher immersion times.

PA, on the other hand, tends to substantially worsen the corrosion behavior of the material since both AS+PA 1M and 14M the potentiodynamic polarization curves are shifted towards lower range of potential and higher range of current density values, meaning that, apart from corrosion susceptibility being greater, corrosion is accelerated. Furthermore, as implied by the recorded i_{pass}, the corrosion rates are far superior to AS and AS+LA. Comparing with the control group, despite $E_{(i=0)}$ being relatively similar, for AS+PA 1M, cp Ti is able form the protective surface film at a lower applied potential, (–0.135 ± 0.245) $V_{Ag/AgCl}$, than the previously discussed solutions.

For a higher concentration of PA (14M), the corrosion behavior is even worse, which can be observed by the shift of the potentiodynamic polarization curve to higher current density values. A new "arm" of values on the potentiodynamic polarization curve, also observed by Singh *et al.* [93]. This branch can be observed between the active region and the passivation plateau. The start point of this new region is the maximum active current density value, also called critical corrosion density (i_c), (111.23 ± 8.15) $\mu A/cm^2$, with corresponding potential called primary passivation potential (E_{pp}), (–0.396 ± 0.014) $V_{Ag/AgCl}$. From this point, there is a rather abrupt current density decrease, indicating that anodic reactions are taking place as a passive film starts to form, until i_{pass}. Here, a well-defined passivation plateau is also observed, and the passive film is formed and stable.

In Singh *et al.* [93] study, cp Ti showed active-passive behavior and a large passivation-plateau when immersed in doubly distilled water with various PA concentrations (1M, 3M, 5M, 9M, 11M and 13 M), at (30±1) °C. The cathodic region was similar for all concentrations, while differences were noted as

$E_{(i=0)}$ was reached. Despite the current density increase with increasing concentration, it only happened from PA 1 to 11M. At PA 13M, the PDP curve is slightly shifted towards lower current density values, where i_c was lower than for PA 9M and 11M and i_{pass} was even lower than for PA 1M. This behavior was attributed to possible changes in the structure of the acidic solution, where a hybride layer was formed by interconnection of PO_4^{3-} ions by hydrogen bonds instead of being bonded to the H_2O lattice. Since not only the base solution is different (doubly distilled water), but the temperature in which the tests were performed is 30 °C rather than 37 °C, the results are not entirely comparable, implying these changes in conditions may cause a completely different outcome.

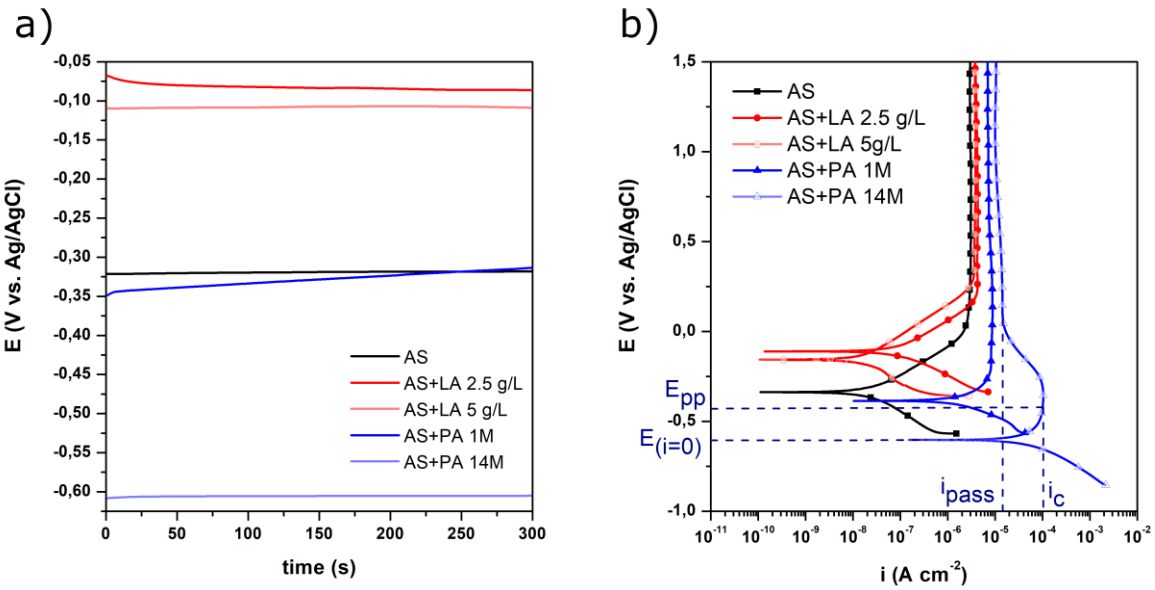

Figure 18 – (a) Evolution of OCP for the last 5 minutes of immersion and (b) potentiodynamic polarization curves of cp Ti for all the electrolytes, at 37°C.

Table 5 - Open-circuit potential (E_{OCP}), corrosion potential ($E_{i=0}$) and passivation current density (i_{pass}) values for all groups.

Groups	E_{OCP} ($V_{Ag/AgCl}$)	$E_{(i=0)}$ ($V_{Ag/AgCl}$)	i_{pass} (μA cm^{-2})
AS	–0.309 ± 0.039	–0.326 ± 0.040	3.32 ± 0.32
AS + LA 2.5 g/L	–0.182 ± 0.085	–0.193 ± 0.070	3.73 ± 0.40
AS + LA 5 g/L	–0.135 ± 0.118	–0.168 ± 0.121	3.85 ± 0.24
AS + PA 1M	–0.311 ± 0.036	–0.328 ± 0.120	7.10 ± 0.70
AS + PA 14M	–0.581 ± 0.061	–0.626 ± 0.021	11.91 ± 1.54

Since the corrosion behavior of a passive metal, such as cp Ti, is majorly determined by the nature of the passive film spontaneously formed on its surface, EIS was performed to have a more complete insight on the differences in corrosion behavior of cp Ti for the various electrolytes. In Figure 19 are represented the EIS diagrams, in the form of Nyquist and Bode, as well as the fitted data and the respective electrical equivalent circuit (EEC).

Overall, the EIS data correlated with the potentiodynamic polarization results. According to the Nyquist diagram, Figure 19 b), when cp Ti is immersed in non-additivated AS it manifested the highest corrosion resistance, due to highest $|Z|_{f \to 0}$. When additives were added to AS, the corrosion resistance of cp Ti decreased: LA 5 g/L > LA 2.5 g/L >> PA 1M >> PA 14M.

The *"depressed semicircles appearance"* in the Nyquist diagrams for AS and AS+LA (2.5 and 5g/L) indicated that the addition of LA did not change cp Ti corrosion mechanism [68].

According to the Bode diagram, Figure 19 a), AS+LA 5 g/L proved to cause great corrosion resistance. At low and middle frequencies (10^{-2} to 10^{1} Hz), not only cp Ti was able to form a compact passive film with good capacitive behavior, due to a broad phase maximum which suggests the formation of a thicker film [70] but phase angle values closer to –90°. Moreover, the overall high system impedance, |Z|, although not as high as the values for non-additivated AS, suggested, once again, the material's high corrosion resistance in this medium. At the same time, at high frequencies, the constant |Z| values and phase angle values near 0° translate the typical response of the electrolyte resistance. For AS+LA 2.5 g/L, although the surface film quality is similar to the films in AS and AS+LA 5 g/L, |Z| is not as high. Qu *et al.* [68] also performed EIS to Ti immersed in AS without and with LA (5 g/L) and it was considered that, overall, LA 5 g/L did not cause a significant difference in the corrosion resistance of Ti. However, SEM images of Ti surface showed that non-additivated AS promotes a smoother surface, since there seen old scratched, and no signs of extreme corrosion and chemical attack were spotted. On the other hand, by adding LA (3.2 g/L and 5 g/L) the authors observed the surfaces tended to look

increasingly damaged with clear signs of pitting corrosion. Such signs of localized corrosion were not observed on the samples surfaces of the present study.

When in contact with PA solution, the metallic samples presented significantly lower corrosion resistance. The Bode diagrams are visibly different from AS and AS+LA, particularly the one for PA 14M, as corrosion resistance is substantially worsened for this concentration (Figure 19 b)). The addition of PA 14M proved to be detrimental to the formation process of a thick and protective layer on the cp Ti surface due to narrower phase maximum angle not as close to –90° the lowest recorded |Z| values of the test, at low and middle frequencies (10^{2} to 10^{1} Hz), as shown in Figure 19 a). At high frequencies (10^{4} to 10^{6}), there was lower constant |Z| values and while phase angle approached 0°, indicating poorer electrolyte response resistance when penetrating a porous film [94].

Moreover, Ghoneim *et al.* [70] study showed compatible results when comparing both concentrations. Triply distilled water with lower concentration of PA (1M) induced overall higher |Z|, broader phase maximum with angles values lose to –90°, at low frequencies, indicating the presence of a thicker and, thereby, more protective film on the surface, relatively to the solution with the highest concentration (PA 14M).

Despite corrosion resistance being significantly worsened by the addition of PA 1M to AS, the data were able to be fitted with a regular compact film model, modified Randle's circuit.

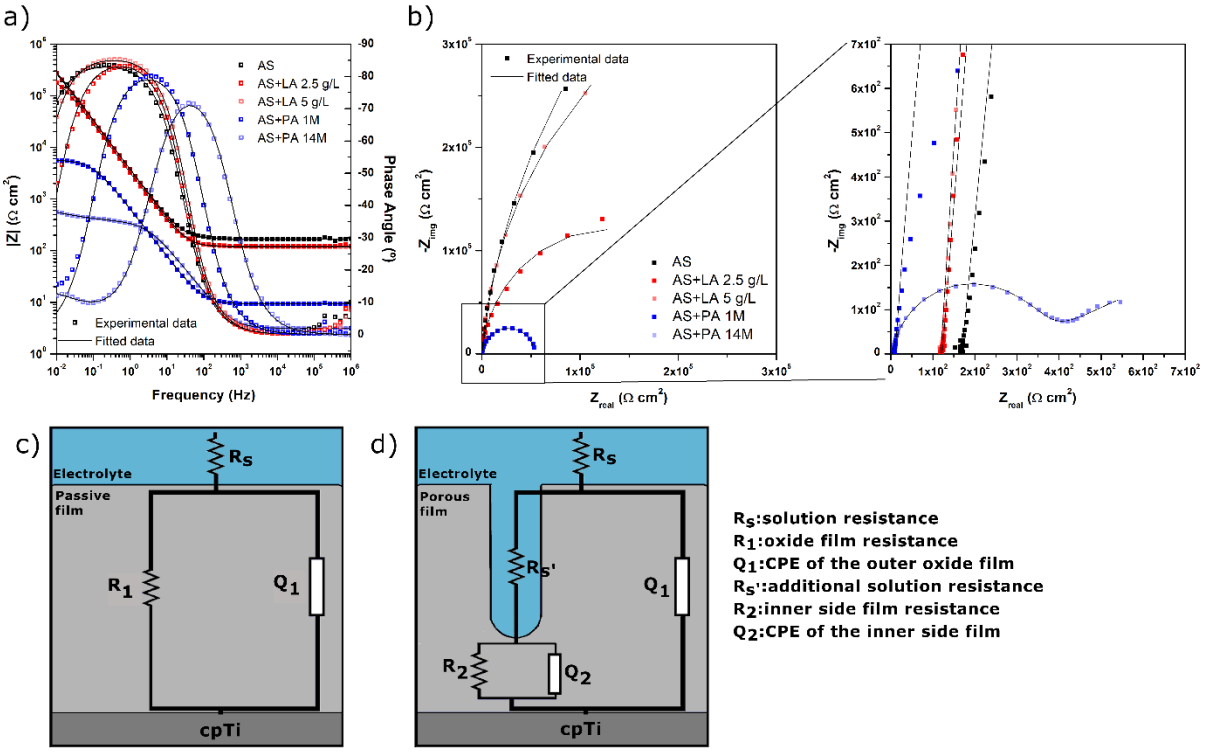

Figure 19 - EIS spectra in the form of a) Bode and b) Nyquist diagrams for all tested conditions, together with the EEC's proposed for c) AS, AS with LA (2.5 g/L and 5 g/L) and AS with PA 1M, and d) AS with PA 14 M, at 37°C.

Figures 19 c) and d) show the schematic representation of the two EEC's used for fitting the EIS experimental data. The EEC in Figure 19 c) is a model that validates the presence of a compact homogenous film (passive state), when cp Ti is immersed in AS, AS+ LA (2.5 g/L and 5 g/L) and AS+PA 1M. This circuit, also known as modified Randle's circuit, widely used in the literature to describe native passive films [64,91,92,95]. This EEC consists in R_s, the solution resistance, in series with a R_1/Q_1 pair, where R_1 is the resistance of the native oxide film, and Q_1, which is a constant phase element (CPE) for the film. The impedance of a CPE is given by Equation (1) [91]:

$$Z(CPE) = [Y_0(jw)^n]^{-1} \quad (1)$$

Where Y_0 is the CPE admittance in $\Omega^{-1}\, s^n\, cm^{-2}$, $j = \sqrt{-1}$ is the imaginary unit number, $w = 2\pi f$ is the angular frequency in $rad\, s^{-1}$ and n is a dimensionless number, being that $-1 \leq n \leq 1$, depending on the surface morphology and composition: for $n = -1$, CPE works as an inductor, $n = 0$ as a resistor, and $n = 1$ as a capacitor . In this case, the obtained n values were approximately 1, confirming the CPE presents a non-ideal capacitor behavior, due to a non-uniform current distribution due to the film roughness and heterogeneities [70,91]. Furthermore, Q_1 is obtained by Equation (2), derived from Brug's equation [92]:

$$C_1 = \left[Q_1 \, R_s^{(1-n)}\right]^{1/n} \quad (2)$$

where C_1 is the capacitance of the oxide film.

On the other hand, the EIS spectra for AS+PA 14M were fitted with a more complex model (Figure 19c)) [64] that implied the presence of a surface heterogeneities or a porous film was present, hence, requiring the introduction of other parameters. This EEC included R_s in series with a parallel combination of Q_1 with a series combination of $R_{s'}$ (additional solution resistance, located in the pores of the film) with a parallel combination of the pair R_2/Q_2 (resistance and CPE located in the inner side of the film), in order to have a better understanding of what is happening in the bulk metal/oxide film interface. Q_2 can be determined through Equation (3), also derived from Brug's equation [92]:

$$C_2 = \left[Q_2 \, (R_s + R_{s\prime})^{(1-n)}\right]^{1/n} \quad (3)$$

where C_2 is the capacitance of the double layer.

The EEC fitting parameters for all solutions are presented in Table 6. The data were found to be adequately fitted to the equivalent circuits, as the quality of fitting was evaluated by the χ^2, for which the EEC presented values under 10^{-3}.

R_s values were decreased by the addition of the additives to AS, since they changed the electrolytes conductivity and enhanced the media corrosivity [64]. The addition of LA led to decreasing R_s with increasing concentration. Although a different EEC was used, Qu *et al.* [68] also concluded the electrolyte resistance decreased with increasing LA concentration (0, 2.5, 3.2 and 5g/L) in AS.

When preparing the electrolytes, the increase in the solution viscosity was visible as PA was added. This certainly reduced the solutions conductivity, leading to the lowest R_s values for AS+PA 14M. Ghoneim *et al.* [70] also used a different EEC, however, when PA 14M was added to triply distilled water also presented lower R_s than for PA 1M.

As expected, non-additivated AS presented the highest R_1, as this film was compact, inhibiting current flow on its surface and keeping the bulk metal passivated. Although not very different, higher R_1 values were obtained for when increasing concentration of LA was added. Despite Qu *et al.* [68] results for LA 5 g/L were not as close to plain AS, they were higher than the values for LA 2.5 g/L. PA 1M, on the other hand, substantially lower R_1 meant that the oxide film became less resistive and, consequently, enabled more current flow through the surface. In the case of AS with higher PA concentration (14M), R_{ct} was used as the term of comparison and, due to five times lower order of magnitude of the results

confirmed cp Ti corrosion resistance in this medium is severely worse. $R_{s'}$ is also to be had taken into consideration and, the extremely lower value when compared to R_1 of the other solutions validates that PA 14M favored active corrosion, causing the film formed on top of cp Ti to self-damage.

Q_1 analysis allows better understanding of the oxide film protection mechanisms [91]. As Q_1 is directly related to C_1 through Equation (2), it is relevant to refer that change in capacitance (C), corresponding to C_1, can be an indicator for the change in the passive film thickness (d). The capacitance is inversely proportional to thickness, according to Equation (4) [70,92]:

$$C = \frac{\varepsilon_0 \varepsilon A}{d} \quad (4)$$

where ε_0 is the vacuum permittivity $(8.85 \times 10^{-12}\ Fm^{-1})$, ε is the relative dielectric constant of the oxide film, being that ε=100 (for TiO_2) and A is the exposed area to the electrolyte. Hence, when C_1 is higher, the film thickness is lower and, consequently, less protection is provided to the bulk metal.

In agreement with the R_{ox} interpretations, the lowest C_1 value was obtained in non-additivated AS, which means that the thickest film was formed in this media. Regarding the addition of LA, as expected, the oxide film formed in AS+LA 5 g/L is thicker than the film in AS+LA 2.5 g/L, hence higher LA concentration can have greater protection to the bulk, as confirmed by Qu *et al.* [68] when immersion time was longer than one hour. PA addition triggered higher C_1 values and obvious thinning of the oxide layer, especially for the highest concentration [70]. In addition to the AS+PA 14M analysis, the high C_2 values, along with C_1, indicated that this electrolyte promoted, indeed heterogeneities in passive film [70]. Hence, film thickness decreased when additives were added to the saliva, particularly PA.

Table 6 - EEC parameters obtained from EIS data for all groups of samples, at 37°C.

Electrolytes	**R_s (Ω cm²)**	**$R_{s'}$ (Ω cm²)**	**C_1 (μF cm^{-2})**	**n_1**	**R_1 (x10^5 Ω cm²)**	**R_2 (Ω cm²)**	**C_2 (μF cm^{-2})**	**n_2**	**χ^2**
AS	164 ± 5	–	35 ± 1	0.93 ± 0.01	7.17 ± 5.10	–	–	–	<10^{-3}
AS + LA 2.5 g/L	126 ± 8	–	43 ± 7	0.95 ± 0.01	4.43 ± 1.66	–	–	–	<10^{-3}
AS + LA 5 g/L	118 ± 5	–	40 ± 13	0.95 ± 0.01	6.21 ± 2.11	–	–	–	<10^{-3}
AS + PA 1M	10 ± 1	–	72 ± 39	0.94 ± 0.02	0.09 ± 0.06	–	–	–	<10^{-3}
AS + PA 14M	3 ± 1	378 ± 94	95 ± 9	0.91 ± 0.01	–	832 ± 4	529 ± 2	0.65 ± 0.06	<10^{-3}

4.2 TRIBO-ELECTROCHEMICAL BEHAVIOR

Dental implants materials must to be able to withstand the mastication forces, while in contact with the saliva and the additives. Hence, the performance of tribo-electrochemical tests on cp Ti, under loaded and reciprocating-sliding conditions, is essential to this study in order to understand the synergistic interactions between corrosion and wear.

4.2.1 TRIBOCORROSION BEHAVIOR UNDER OCP

4.2.1.1 OCP AND COF EVOLUTION

Figure 20 shows the evolution of the OCP before, during and after the sliding action, together with the evolution of COF. In the beginning of the test, all samples presented a stabilized OCP, indicating that a passive oxide film was formed.

Regarding the OCP results, as soon as loading and sliding started, almost instantly, the cp Ti samples immersed in AS and AS+LA (2.5 and 5g/L) demonstrated an abrupt decrease in OCP, also called cathodic shift, due to the mechanical disruption and/or destruction of the surface film by the Al_2O_3 ball, leading to the exposure of fresh metal to the electrolyte. In other words, corrosion susceptibility increased, however, after this potential drop, potentials reach a steady state, where oscillations can be observed due to the cyclic removal (depassivation) and restoration of the film (repassivation) [33,34,91,96]. It is reported that these variations may also be caused by the abrasion of wear debris against the metallic surface, causing even more damage to the film [33]. Cp Ti showed the worst tribocorrosion behavior for AS. Hence, due to the higher OCP values, during sliding, the addition of lactic acid proved to have protective-like role for cp Ti, when subjected to mechanical action. For the highest concentration (5 g/L), the behavior is slightly improved, when comparing to LA 2.5 g/L, due to the higher OCP, values during sliding. Finally, when sliding stopped, the OCP presented a sudden increase close to the pre-sliding values, for each electrolyte, which was attributed to the complete repassivation of the worn areas [33,91,95,96].

The addition of phosphoric acid to artificial saliva showed intricate results during sliding. Overall, cp Ti presented the best tribocorrosion behavior when PA 1M was added to artificial saliva due to the no observation of an abrupt cathodic shift, in the beginning of sliding, and almost no potential fluctuations, during sliding. As mentioned before, during the preparation of the electrolytes, when compared with AS and AS+LA solution, increasing PA content in AS visibly increased viscosity of the solution. In fact, phosphorus (P) is a known constituent of anti-wear (AW) and extreme pressure (EP) additives for lubricant

applications so that friction and, therefore, wear are reduced [97]. Thus, despite the thin passive film showed in static conditions, the fact that PA 1M worked as a lubricant during sliding caused almost no disturbance of the passive film and a minimal effect on the low corrosion susceptibility of cp Ti, during the mechanical action. After the end of sliding, the almost non-repassivation of the surface is supported by the fact that no great damage was inflicted to the passive film by the mechanical action and that, in agreement with the EIS tests, a poor resistive film was covering the surface, meaning that corrosion susceptibility of cp Ti was minimally affected.

On the other hand, a visibly worse tribocorrosion behavior was shown when cp Ti was in contact with AS+PA 14M. In this case, OCP had a straight-line appearance, where the pre-sliding OCP values were constant throughout the entire test. Through the OCP, PDP and EIS tests of the present study, it was possible to conclude that unworn cp Ti was in its active state, during static corrosion, due to AS+PA 14M harshness and the porosity of the thin passive film formed on its surface. Hence, this phenomenon, also reported by Sousa *et al.* [33] when testing cp Ti with a highly fluoride concentrated (12 300 ppm) Fusayama's artificial saliva, combined with the powerful lubricant effect induced by PA 14M, explained cp Ti low corrosion susceptibility not being at all affected by sliding. When sliding stopped, nothing different occurred and the OCP values remained constant.

Furthermore, it is reported the potential increase (ΔE) (V), that characterizes the metal repassivation after sliding, can be calculated through the tangent equation in the beginning of the repassivation process [98–100]:

$$\Delta E = k_1 \log t + k_2 \quad (5)$$

where k1 is the slope of the equation and, therefore, the repassivation rate, in this case, calculated for a period of 300s after the end of sliding, t (s) is the time after interrupting sliding, 300s, and k2 is a constant, as is k1, calculated by fitting the OCP values, after sliding, to Equation (5).

In Table 7 are presented k1, k2 and ΔE. These results showed that, despite the poor tribocorrosion behavior exhibited by cp Ti in AS, this solution promoted the greatest repassivation rate, meaning that repassivation was faster in non-additivated AS. Hence, in accordance with the OCP results, the addition of additives decreased cp Ti repassivation rate: AS+LA 5 g/L > AS + LA 2.5 g/L >> AS+PA 1M. Since no repassivation was noticed for cp Ti when immersed in AS+PA 14M, the respective parameters are not included in Table 7.

Table 7 - ΔE, k1 and k2 parameters for repassivation rate calculations.

	k_1 (V/s)	k_2	ΔE (V)
AS	0.156 ± 0.013	−0.036 ± 0.043	0.350 ± 0.013
AS+LA 2.5 g/L	0.111 ± 0.016	−0.026 ± 0.032	0.250 ± 0.009
AS+LA 5 g/L	0.143 ± 0.030	−0.013 ± 0.035	0.341 ± 0.103
AS+PA 1M	0.007 ± 0.001	−0.004 ± 0.003	0.014 ± 0.004

Regarding the COF results, there is an evident correlation with the OCP oscillations during sliding. AS and AS+LA (2.5 and 5 g/L) showed relatively similar and stable COF values, with 0.48 ± 0.02, 0.46 ± 0.03 and 0.48 ± 0.04, respectively. This friction evolution can be attributed to high abrasion for these electrolytes, by possible surface delamination and the formation of bigger-size wear debris [91].

According to Ponthiaux *et al.* [75], COF *"depends on the electrochemical state of the material"* and the level of protection provided by the passive film, however, despite the poor corrosion behavior and the formation of thin passive films, lower number of variations and COF were presented by PA-based electrolytes, mainly due to the higher viscosity and, hence, their lubricant effect on the mechanical sliding. For AS+PA 1M, cp Ti showed COF of 0.43 ±0.04 and even lower for AS+PA 14M (0.39 ±0.04).

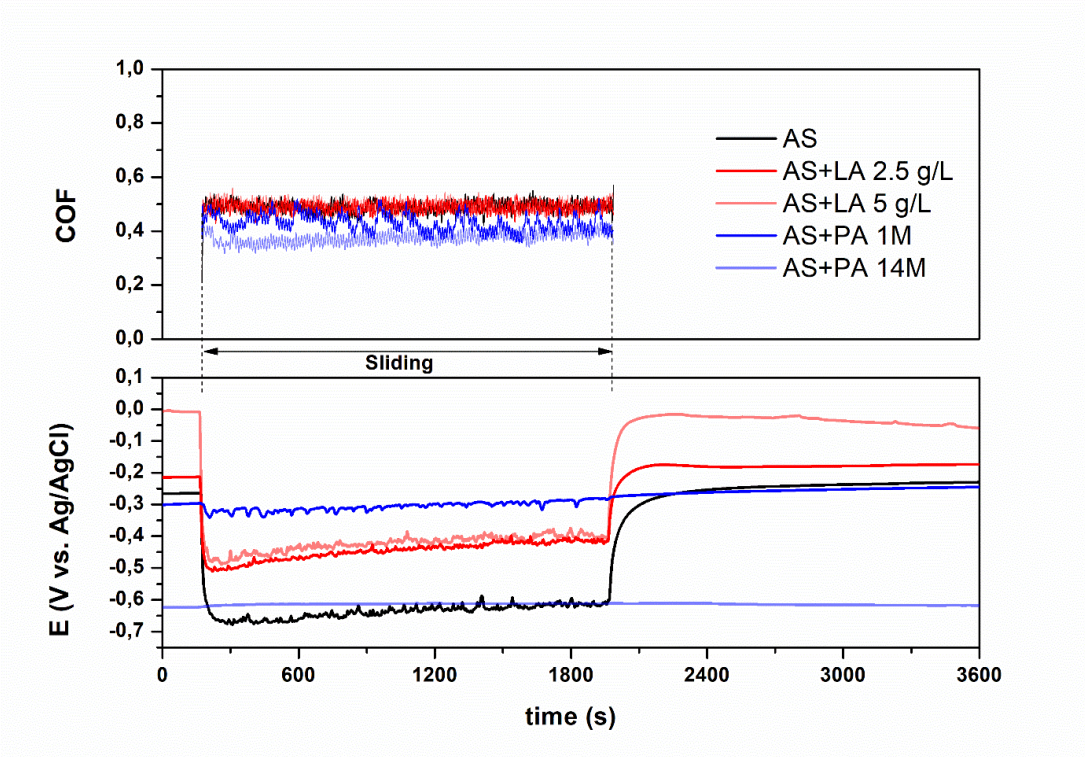

Figure 20 - OCP evolution before, during, and after sliding, together with the evolution of COF, during sliding, for all tested groups, at 37°C.

4.2.1.2 CHARACTERIZATION OF THE WORN SURFACES AND WEAR MECHANISMS

Representative optical microscope images of the wear tracks and SEM/EDS of the worn cp Ti surfaces and respective Al_2O_3 counter part (Figure 21) were taken in order to thoroughly investigate the tribocorrosion mechanisms.

Sousa *et al.* [33] reported the alignment of the wear scar marks with the sliding direction when cp Ti was immersed in Fusayama's artificial saliva. In the present study, this could be observed for all five groups as an indicator of abrasive mechanisms [91].

In agreement with tribo-electrochemical results, the OM images proved that the immersion in AS caused the largest wear tracks, with a width of (712 ± 22) μm, followed by AS+LA 2.5 g/L and AS+LA 5 g/L, with (692 ± 23) μm and (694 ± 16) μm, respectively. For these three conditions, the SEM images of the wear tracks revealed clear signs of parallel ploughing grooves (plastic deformation) and surface material detachment, due to abrasion and adhesion mechanisms [90,95]. It is also important to note that oxidized patches could be observed for these three conditions, in BSE images. These mechanisms were more noticeable in the presence of non-additivated AS.

The formation of third-body particles (wear debris from adhesion and/or corrosion wear) along with this material detachment are reported to cause more variations on COF, as well as having a decisive role for mechanical wear [33]. These metallic particles might be oxidized and it severely increase in the tested material wear loss, or it can act as a lubricant, inhibiting friction between surfaces and therefore, wear [34,101]. In the case of AS, due to intense material transfer, these wear debris tend to be oxidized and harden causing detrimental effects to mechanical wear [90].

Furthermore, for AS+LA solutions, a dark mark of oxide debris can be observed around the wear track, suggesting that oxide products were ejected from the surface to the electrolyte, and then mainly deposited around the worn area. The COF of cp Ti in AS+LA solutions was similar to AS, however, more positive OCP values, thus, better behavior was noticed during sliding, suggesting the increased concentration of lactic acid induced new reactions, possibly related to the wear debris that provided a certain protection to cp Ti [71].

The EDS spectra of the worn areas of the wear tracks were similar for AS and AS+LA (2.5 and 5 g/L), where Ti was understandably the predominant element, followed by the characteristic peak for Ti and O, which are elemental constituents of the previously formed passive film. Other elements, such as phosphorus (P) and chlorine (Cl) were detected as they were part of the elemental constitution of the base electrolyte, artificial saliva.

For both AS and AS+LA, adhesion mechanism is mainly associated with Ti high reactivity [90], it was evident not only due to the ploughing grooves formation in cp Ti surfaces, but also to the transferred material from the softer surface (cp Ti) to the harder one (Al_2O_3 ball). The wear scars on the Al_2O_3 balls were the largest for non-additive AS, which is in accordance with size of the wear tracks. The EDS spectrum for AS confirmed the detection of Ti at a very high ratio. For the addition of LA, on the other hand, despite the close size wear tracks to the ones for AS, the wear scars in the counter-body were smaller and had a different appearance, especially for the higher concentration of LA (5g/L). In these cases, the EDS spectra were similar and proved adhesion was also a factor for AS+LA solutions due to the transference of Ti.

Taking into consideration that no cathodic shift on OCP when sliding started and the lower COF values during sliding, OM images confirmed that AS+PA 1M and AS+PA 14M induced the smallest contact areas on cp Ti, with and average width of (317 ± 6) μm and (315 ± 2) μm, respectively. This phenomenon is directly linked to the lubricant effect provided by the presence of P, causing less wear to the surfaces. For the lowest concentration (1M), SEM analysis showed scratches on the cp Ti surfaces, which is an indicator of abrasion and material detachment in certain areas were observed, with no apparent plastic deformation. In this case, EDS also displayed the peak for the detection Ti and O. Regarding the respective counter-body, a small scar was observed, suggesting less adhesion, however, some dark patches were observed that EDS spectrum demonstrated they consisted in oxidation products and Ti, that were transferred to the ball.

Lastly, for AS+PA 14M, surface wear was strongly dominated by fatigue due to the appearance of small numerous fissures along the abrasion scratches. For these surfaces, the detection of Ti and O peaks were also observed. Fatigue wear can occur even when lubricants are present, since the tensions are still transferred to the tested material [102]. It is also reported that, even in well lubricated conditions, significant amount of wear could happen despite minor adhesion [103]. In fact, for AS+PA 14M, a scar was not visible in the counter-body with SEM and a negligible amount of Ti was detected in the alumina ball. Even more evidently than AS+PA 1M, the highest PA concentration lubricated the contact between cp Ti and the counter-body, yet wear, however lower than other conditions, still occurred. Moreover, for both PA concentrations electrolyte constituents were detected on the cp Ti surfaces.

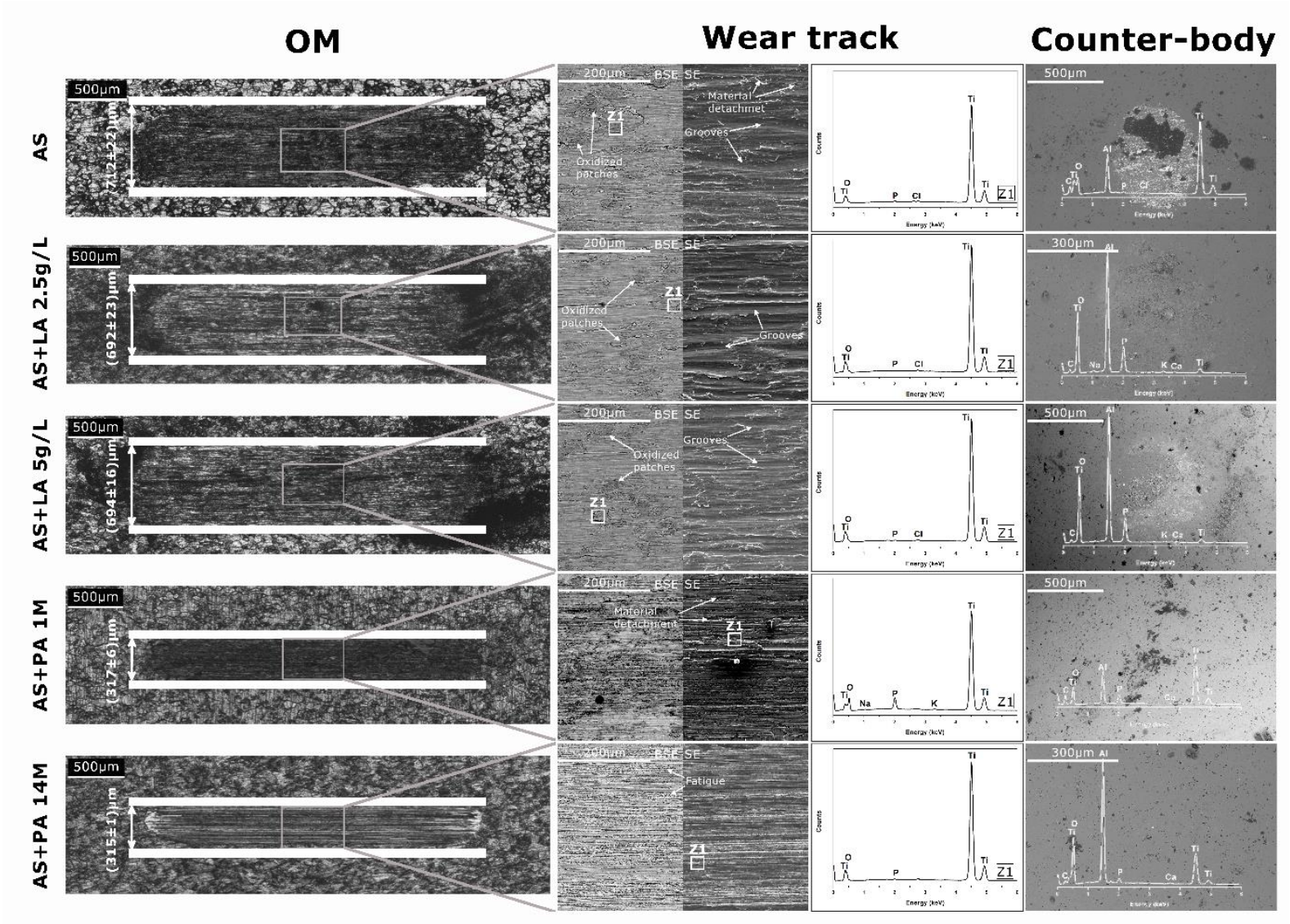

Figure 21 - OM, BSE and SE-SEM images of the wear track and the respective EDS spectra, and SEM and EDS of the counter-body, for all groups, after the tribo-electrochemical tests at OCP

4.2.2 AT +0.5$V_{AG/AGCL}$

For the proposed solutions, cp Ti presented significant dissolution through oxidation reactions, so a synergism between corrosion and wear is irrefutable. This emphasizes the relevance of the performance of potentiostatic tests with an applied anodic potential of +0.5$V_{Ag/AgCl}$, located in the passive zone for all electrolytes.

4.2.2.1 POTENTIOSTATIC MEASUREMENTS

Figure 22 shows the evolution of the anodic current density (i) before, during and after the sliding action, together with the evolution of COF. At the end of the first 10 minutes of the test, all samples presented a stabilized current density around (0.47 ± 0.93) µA.cm^{-2} for AS, (-0,07± 0.93) µA.cm^{-2} for AS+LA (2.5 and 5 g/L) and AS+PA 1M, and (1.21 ± 0.40) µA.cm^{-2} for AS+PA 14M.

Regarding the current density results, when loading and sliding started, almost instantly, the cp Ti samples for all electrolytes demonstrated an abrupt increase in anodic current density due to the mechanical disruption and/or destruction of the surface film by the Al_2O_3 ball, leading to the exposure of fresh metal to the electrolyte and, hence, increasing corrosion kinetics [90,104]. When load was applied, the highest increment in current density was recorded in the presence of non-additivated AS. After this current density increase, fluctuations of current density values were observed, as a sign of cyclic removal (depassivation) and restoration of the film (repassivation), during sliding. Similarly to the oscillations on the tribo-electrochemical results at OCP, these fluctuations of current density may also have been caused by the abrasion of wear debris against the metallic surface, causing even more damage to the film [33].

Cp Ti showed the greatest current density value and the greatest current density fluctuations for AS+LA 5 g/L, indicating considerable surface damage [85]. Thus, the slightly lower current density values, especially towards the end of sliding, for non-additivated AS and AS+LA 2.5 g/L suggested that the passive film provided better protection to the bulk.

On the other hand, PA-concentrated solutions presented the lower current density values, probably due to the lubricant effect of the electrolyte. However, when comparing the results for both PA concentrations, AS+PA 1M presented mixed peaks of higher and lower current density values at some stages of sliding, in sync with COF variations. According to Sousa *et al.* [90], this phenomenon could be related the formation a *"discontinuous tribolayer"* that protected the metal, and lowered current density, in certain areas against wear and corrosion. It may be speculated that this layer could be similar to the hybride layer reported by Singh et al. [93], considering that, their study, 30°C and a less P-enriched base

electrolyte (doubly distilled water) was used. Hence this layer could already start its formation on cp Ti surface at a lower PA concentration than it was reported (13M). AS+PA 14M, on the other hand, presented relatively stable current density, with smaller and homogenously distributed peaks throughout the sliding period than AS+PA 1M, and slightly higher current density values. This behavior could be attributed to the strong lubricating capacity and high corrosivity of this electrolyte, proven through the potentiodynamic polarization and EIS tests.

Finally, when sliding stopped, the current density presented a sudden decrease to similar pre-sliding stabilization values, for each electrolyte, which was attributed to reinstatement of the passive film in the worn areas [104].

Regarding the COF results, there is an evident correlation with the current density variations during sliding. Similarly to tribo-electrochemical test results at OCP, AS and AS+LA (2.5 and 5 g/L) solutions exhibited the highest COF values: 0.44 ± 0.02, 0.44 ± 0.03 and 0.44 ± 0.02, respectively. High COF values are usually linked to abrasion and material detachment and the formation of wear debris that promote friction between the first and second bodies [91].

Furthermore, AS+PA solutions led to lower COF values. Despite the overall lower COF by AS+PA 14M (0.34 ± 0.02), which is the most viscous electrolyte, when comparing with AS+PA 1M (0.37 ± 0.04), at certain stages of sliding, the lowest PA concentration induced lower friction. As mentioned before, this could be seen as a sign of a protective layer that is cyclically formed (low current density) and destructed (high current density).

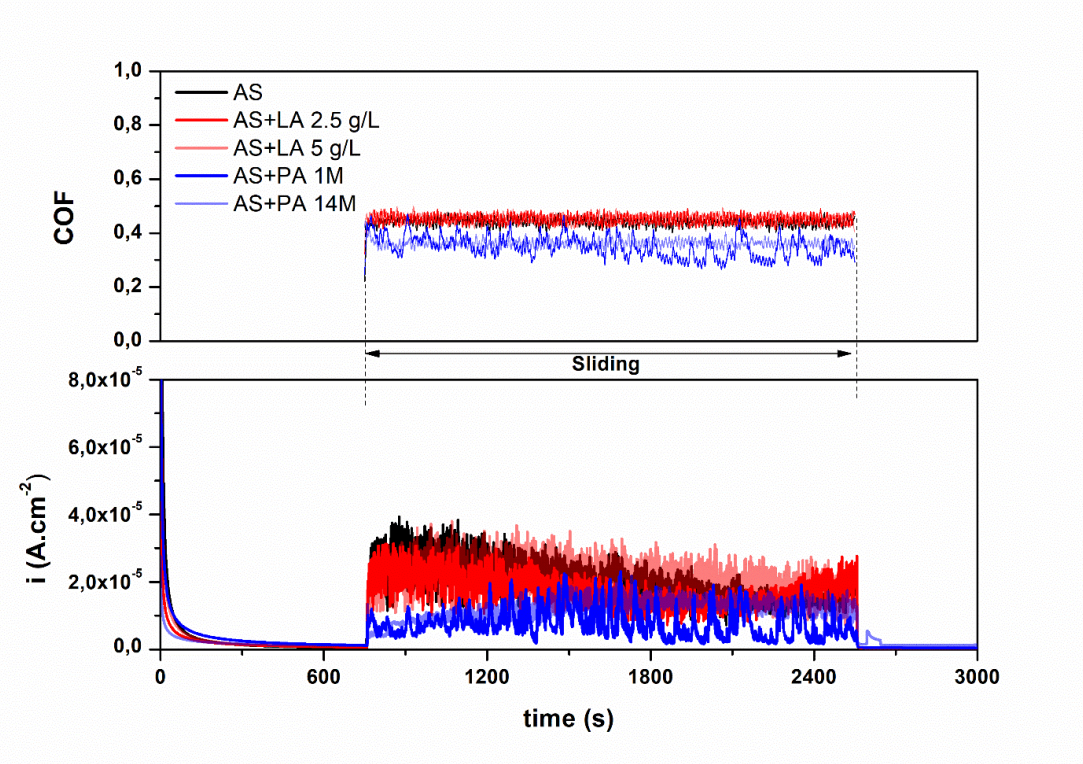

Figure 22 - Representative current density evolution before, during, and after sliding, along with the evolution of COF, during sliding, at 37°C.

4.2.2.2 CHARACTERIZATION OF THE WORN SURFACES AND WEAR MECHANISMS

OM and SEM/EDS were equally performed to the worn cp Ti surfaces and respective Al_2O_3 ball, after the potentiostatic tests, to gather further information regarding cp Ti surface wear, as well as its mechanisms, for all electrolytes. The representative images are presented in Figure 23.

Similarly to tribo-electrochemical tests at OCP, alignment of the wear scar marks with the sliding direction was observed for all groups, as a sign of abrasive mechanisms [91].

Optical microscope images showed that, overall, wider wear tracks were formed in potentiostatic conditions. This behavior could be attributed to the fact that, despite reports of increasing film quality and thickness when higher potentials are applied [105], the anodic film may consist of different structured oxides. In other words, the nature of both films, at OCP and $+0.5V_{Ag/AgCl}$, is same, however, when forcing a film to be formed by applying the anodic potential, leading to different thickness of the natural film formed during 3h of OCP monitorization. Hence, when this film is disrupted/destroyed, greater volume loss could be noted.

Again, the largest tracks were promoted by the presence of non-additivated AS, with (749 ± 20) µm, while AS+LA (2.5 and 5 g/L) induced tracks of (735 ± 15) µm and (732 ± 13) µm, respectively. SEM images showed abrasion and adhesion phenomena, with highly noticeable plastic deformation

through parallel ploughing grooves, as well as larger-sized gaps where material detached from the surface, when comparing with the results at OCP. Oxidized patches were identified as well. According to Silva *et al.* [106], these compacted oxidized debris could cause a dual effect: localized protection could be provided to the testing material, as a consequence of their higher hardness, or the formation of third-body particles could happen and, therefore, increase abrasion between the surfaces. It was also reported that, at a normal load of 1N, oxidized patches were relatively looser from the surface than for higher load (10N) [106]. Hence, taking into consideration the larger tracks for non-additivated AS and the large amount of collect debris, the second option appears to be the most plausible. From EDS analysis it was detected the presence of Ti, as well as other elements constituent of AS.

In AS+LA solutions, cp Ti suffered slightly less plastic deformation than in non-additivated AS. However, at LA 2.5 g/L signs of material detachment were found, contrary to the tribo-electrochemically tested samples at OCP. In fact, despite similar COF values for these three conditions, the anodic current density evolution on cp Ti pointed the LA-enriched solutions to have very close behavior to AS, when potential was applied, suggesting that, in potentiostatic conditions, the corrosion rate is increased and closer to cp Ti in AS. In fact, AS+LA 5 g/L current density was overall higher than AS and AS+LA 2.5 g/L, which could suggest a more considerable effect of corrosion in cp Ti material damage [85] and/or, since the dark mark of oxide debris is no longer located around the wear tracks, it may be speculated that the deducted protection provided by those debris at OCP was inhibited when the anodic potential was applied to the samples. EDS spectra of cp Ti in contact AS+LA (2.5 and 5 g/L) showed similar results to those of AS, by detecting peaks for Ti, and Ti and O.

Comparing Al_2O_3 balls for these three conditions, in agreement with the wear track sizes, abrasion marks were more visible in the presence of AS, followed by AS+LA 2.5 g/L and AS+LA 5g/. EDS proved the material transfer to the balls (adhesion) [90], for the three electrolytes, with AS promoting higher peaks of Ti. When comparing with the counter-body scars formed during tribo-electrochemical tests at OCP, these three electrolytes promoted bigger scars, suggesting that higher volume losses in potentiostatic conditions.

Regarding the counter-body surfaces, a lighter scar was detected for AS+PA 1M, when comparing with tribo-electrochemical tests at OCP, with EDS spectrum detecting, once again, Ti and O, along with a high peak of P. For the highest PA concentration, no scar was detected on the Al_2O_3 ball and no detection of Ti and O was presented. Thus expected, significantly less and smaller wear debris were collected from the wear tracks as PA was added, confirming decreasing wear volume loss promoted by the lubricant effect of PA.

Wear debris were collected with carbon tape from the cp Ti samples. Flakier-looking debris were formed as LA concentration increased, which may be a sign of delamination and explain the high current density values, since these third-body particles increase abrasion, causing more critical damages to the surface [91]. Besides this, when immersed in AS, cp Ti produced a more substantial amount of, as described by Çaha *et al.* [91], "blocky debris" along with some bigger-sized wear particles ~ 50 μm were found on cp Ti wear tracks.

Regarding the addition of PA to AS, the lower additive concentration induced lower width-sized wear tracks than AS and AS+LA solutions: (375 ± 9) μm for AS+PA 1M and (370 ± 10) μm for AS+PA 14M. As mentioned before, this, along with the lower COF and current density values might be linked to the lubricant properties promoted by increasing presence of phosphorus [97]. SEM images for the lowest PA concentration revealed signs of abrasion and adhesion, together with localized formation of a new layer. Singh *et al.* [93] reported the formation of a hybride layer for 13M PA in doubly distilled water, triggered by PO_4^{3-} adsorption capacity to cp Ti. Hence, for 1M light adsorption phenomena could have been taking place so that an easily disturbed layer was formed, considering the current density and COF oscillations. In agreement with these assumptions, for AS+PA 14M, a similar structured layer appeared to be fully formed on the cp Ti surface, with some localized damages of this layer, that may be attributed the combination of the mechanical action and the high corrosivity of this medium. Furthermore, EDS spectra for both concentrations revealed peaks for Ti and oxidation products, as well as more defined peaks for P, supporting the theory the hybride layer.

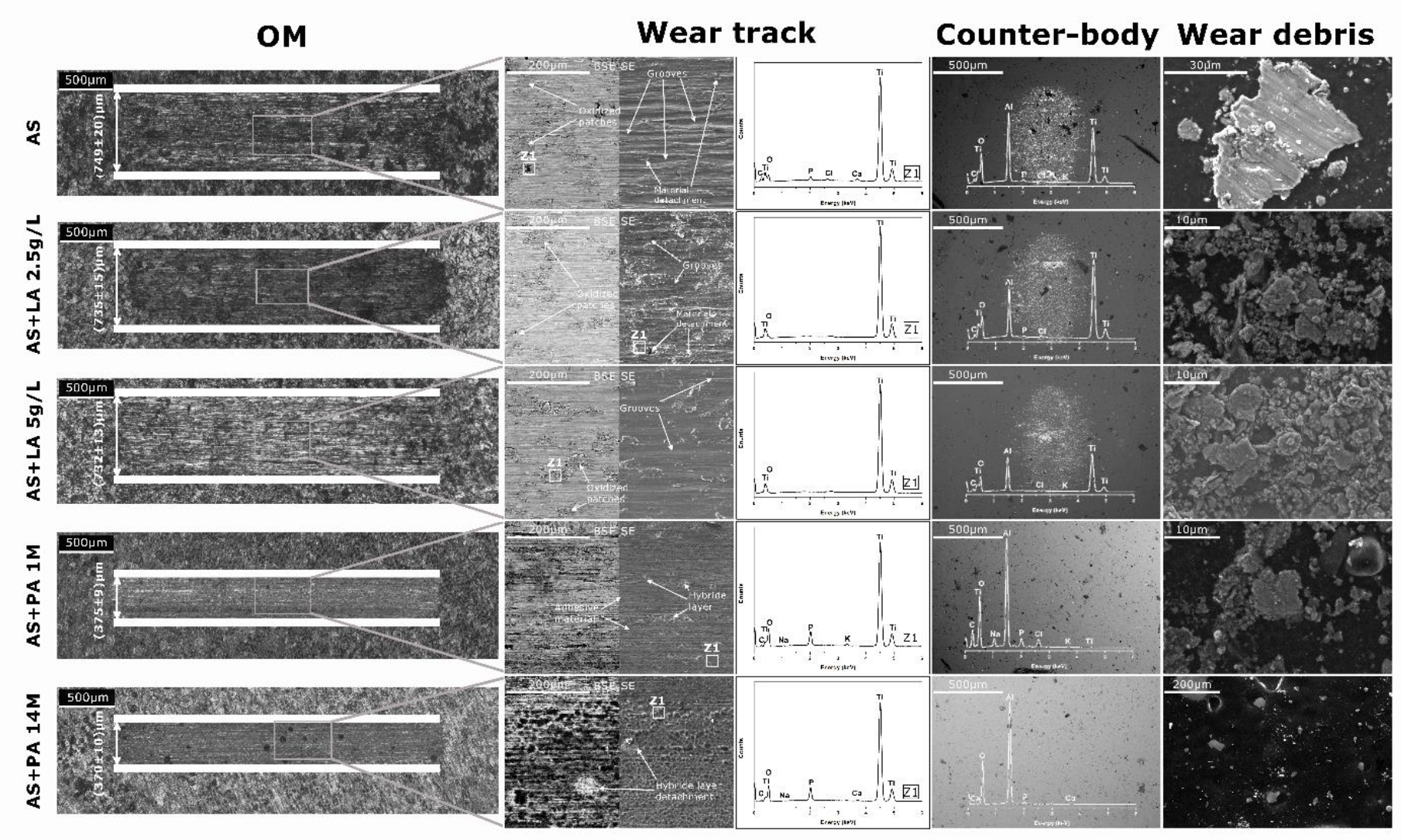

Figure 23 - OM, BSE and SE-SEM images of the wear track and the respective EDS spectra, and SEM and EDS of the counter-body, for all groups, after the tribo-electrochemical tests at OCP.

4.3 COMPARISON OF WEAR VOLUME LOSS BETWEEN THE TRIBO-ELECTROCHEMICAL TESTS AT OCP AND +0.5$V_{Ag/AgCl}$

Further analysis of the wear tracks was carried to have a better understanding of the effect of the electrolytes on cp Ti surface topography and properties, inside and outside the wear tracks, and therefore, compare tribocorrosion behavior at OCP and +0.5$V_{Ag/AgCl}$. For that end, for all electrolytes, the wear profiles and wear volume losses were measured by profilometry, as well as surface roughness and hardness inside and outside the wear tracks.

In order to clarify the contribution of corrosion and wear, the mechanistic approach, reported by Mischler *et al.* [84], was adopted for the quantification of both mechanical wear and wear-accelerated corrosion mechanisms, in potentiostatic conditions, through Equation (6):

$$V_{total} = V_{chem} + V_{mech} \quad (6)$$

where V_{total} is the total wear volume, and V_{chem} and V_{mech} correspond to the wear volumes promoted by corrosion and mechanical action, respectively. V_{total} (Figure 24) was obtained by through measurements of the wear profiles and V_{chem} were estimated by Equation (7) [104]:

$$V_{chem} = \frac{Q \times M}{n \times F \times \rho} \quad (7)$$

where M is the atomic weight of the dissolving element, Ti, (47.867u), n is the valence number of Ti (+4), F is the Faraday constant (96490 C mol^{-1}), ρ is the specific weight of the wore material, cp Ti Grade 2, (4.5 g cm^{-3}) and Q is the electric charge, calculated through integration of the current (I) for the sliding period, as shown in Equation (8) [84,104]:

$$Q = \int_0^{t_{sliding}} I(t)dt \quad (8)$$

Hence, V_{chem} values, and thus, V_{mech} were determined for all conditions, since V_{total} was already know by profilometry measurements (Figure 24). Mathew *et al.* [85] reported criteria (Table 8) that allowed the evaluation of the dominant degradation mechanism of the total wear volume loss, by comparing V_{chem}/V_{mech} ratios for the testing conditions.

Table 8 - Criteria to determine the dominant degradation mechanism of the total wear volume loss [85].

Synergistic ratio	Degradation mechanism
$V_{chem}/V_{mech} \leq 0,1$	Wear
$0,1 < V_{chem}/V_{mech} < 1$	Wear-corrosion
$1 < V_{chem}/V_{mech} \leq 10$	Corrosion-wear
$V_{chem}/V_{mech} > 10$	Corrosion

According to the results presented in Table 9, it was possible to conclude that degradation of cp Ti in non-additivated AS was wear-dominated, as V_{chem}/V_{mech} was below 0.1. In fact, according to OM and SEM images, wear tracks on cp Ti and scars on Al_2O_3 balls were more noticeable for AS due to clearer signs of abrasion, adhesion, material detachment and plastic deformation. When additives are added, $0.1 < V_{chem}/V_{mech} < 1$, indicating synergistic effect between material dissolution reactions (corrosion) and mechanical wear on cp Ti degradation.

Table 9 - Chemical and mechanical wear volume losses, during the potentiostatic tests.

Electrolytes	V_{chem} (10^{-3} mm^3)	V_{mech} (10^{-3} mm^3)	V_{chem}/V_{mech}
AS	0.96 ± 0.14	10.37 ± 0.49	0.09
AS + LA 2.5 g/L	0.89 ± 0.16	8.25 ± 0.11	0.11
AS + LA 5 g/L	1.14 ± 0.20	7.13 ± 0.07	0.16
AS + PA 1M	0.43 ± 0.11	3.04 ± 0.50	0.14
AS + PA 14M	0.49 ± 0.07	2.39 ± 0.2	0.20

Thus, by applying a passive potential, the film formed on cp Ti might not be able to achieve the same thickness, and, the same level of protection to the bulk, as the 3 hour-long naturally formed films. This could explain the overall larger wear tracks (Figure 24), and therefore, higher wear volume (Figure 24), obtained under anodic potential application, for all electrolytes.

In agreement with previous analysis, AS was the electrolyte that induced the largest and most worn tracks on cp Ti, as wear had a key role on material degradation. For AS+LA solutions, the metallic samples showed not considerably smaller wear tracks, hence, slightly lower wear volume losses as LA was added to AS. Important to note that, in agreement with the current density measurement, when the anodic potential was applied, wear volume for AS+LA solutions was even closer to the wear volume in non-additivated AS, which could be attributed to the formation "flake-like debris" that increased abrasion

and the no longer presence of the oxide debris mark around the wear tracks, that may have protected the surfaces at OCP [91].

PA solutions produced, for both types of tests, the lowest wear volumes and the visibly narrower and less deep wear tracks due to the increasing viscosity of the media with increasing PA concentration. At +0.5 $V_{Ag/AgCl}$, higher wear volume was measured, which could be attributed to possible enhancement of corrosion and/or wear, triggered by the "bubbled layer".

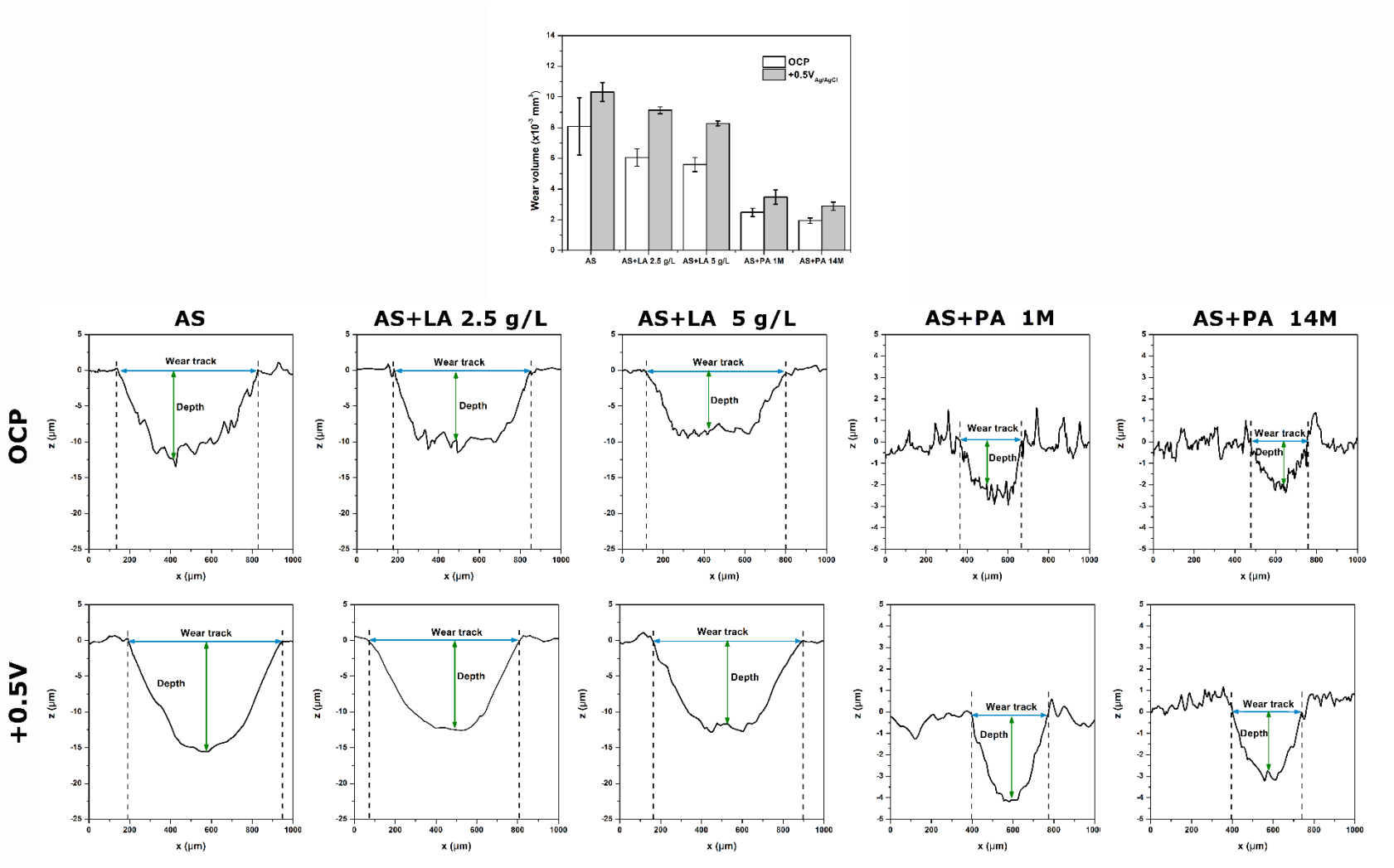

Figure 24 - Wear volumes and representative 2D wear track profiles of the cp Ti worn surfaces for all electrolytes, after tribo-electrochemical tests at OCP and +0.5$V_{Ag/AgCl}$, at 37°C.

.

When sliding a hard-rough material, such as Al_2O_3 against cp Ti, abrasion of the passive film is the ruling wear mechanism so that surface roughness on the contact areas of the softest materials are modified and depassivation and mechanical wear rates are severely affected. Thus, COF is also conditioned by the surface roughness of the contacting materials [38,90].

Surface roughness (R_a) measurements are given in Table 10. All electrolytes promoted higher R_a inside the wear tracks, at both OCP and $+0.5V_{Ag/AgCl}$. In accordance with COF values, AS and AS+LA solutions were the electrolytes that induced overall rougher surfaces, as result of abrasion and material detachment [91]. PA solutions, on the other hand, induced lower surface roughness on cp Ti, for which the main reason may be the less contact between the samples and the balls, promoted by the viscosity of the solutions.

Interestingly, despite the larger wear tracks and higher wear volumes under potentiostatic conditions, rougher surfaces inside and outside the wear tracks were presented after tribo-electrochemical tests at OCP, as confirmed by the slightly lower COF values at OCP. This phenomenon could be attributed to overall higher material dissolution, and therefore, more a more intense synergism between corrosion and wear, when anodic potential was applied, together with the fact that the anodic films might not be as thick as the naturally formed ones, so that the bulk metal was more easily disturbed.

Table 10 - Average roughness values (R_a) of cp Ti surfaces, after tribo-electrochemical tests at OCP and potentiostatic conditions.

Electrolytes	**Ra (µm)**			
	OCP		**+0.5V**	
	Inside	**Outside**	**Inside**	**Outside**
AS	1.32 ± 0.37	0.95 ± 0.44	0.66 ± 0.16	0.20 ± 0.12
AS + LA 2.5 g/L	0.96 ± 0.23	0.55 ± 0.06	0.67 ± 0.26	0.34 ± 0.16
AS + LA 5 g/L	1.11 ± 0.26	0.51 ± 0.11	0.70 ± 0.28	0.25 ± 0.05
AS + PA 1M	0.40 ± 0.11	0.34 ± 0.11	0.42 ± 0.11	0.25 ± 0.11
AS + PA 14M	0.30 ± 0.10	0.31 ± 0.13	0.41 ± 0.08	0.22 ± 0.13

Vickers hardness (HV) was also measured (Table 11). Similar to Ti-6Al-4V, in Çaha *et al.* [91] study, cp Ti showed higher hardness inside the wear tracks, for all electrolytes. These phenomena were attributed cold-hardening phenomenon, due to plastic deformation and material dislocation and

compaction with ongoing sliding. Hence, as expected, the hardest wear tracks belonged to AS, and decreased with increasing concentration additives: LA 2.5 g/L > LA 5 g/L > PA 1M > PA 14M.

As previously noted, as a result of intense material transfer, wear debris could tend to oxidize and harden [90,106]. In fact, at OCP, higher hardness values were measured which could be directly caused by the relatively higher number of oxidized patches. The same reasoning could be applied when comparing material hardness for AS and AS+LA solutions to AS+PA, where no oxidized patches were noticed.

Moreover, besides higher HV and the formation of oxidized patches, the lower volume loss at OCP could be linked to plastic deformation at subsurface of the wear track [91].

Table 11 - Vickers Hardness ($HV_{0.5}$) of cp Ti, after the tribo-electrochemical tests at OCP and potentiostatic tests.

Electrolytes	**Vickers Hardness ($HV_{0.5}$)**			
	OCP		**+0.5$V_{Ag/AgCl}$**	
	Inside	**Outside**	**Inside**	**Outside**
AS	201 ± 7	163 ± 11	213 ± 7	159 ± 9
AS + LA 2.5 g/L	201 ± 9	170 ± 2	192 ± 6	159 ± 9
AS + LA 5 g/L	194 ± 5	165 ± 7	179 ± 11	172 ± 6
AS + PA 1M	189 ± 6	166 ± 9	209 ± 9	166 ± 8
AS + PA 14M	183 ± 4	167 ± 3	206 ± 7	172 ± 5

5 CONCLUSIONS AND FUTURE WORKS

5.1 CONCLUSIONS

In this study, the effects of additives in artificial saliva on the corrosion and tribocorrosion behavior of cp Ti (grade 2) were investigated.

Cp Ti presented overall the best corrosion behavior when in contact with non-additivated AS due to the presence of a more compacted and thicker passive film. Lactic acid proved to not have a significant effect on the corrosion behavior, while phosphoric acid-concentrated AS promoted significantly lower corrosion resistance.

After tribo-electrochemical tests, at OCP and $+0.5V_{Ag/AgCl}$, non-additivated AS induced larger wear tracks and higher wear volume loss than additivated solutions. For simple AS, the mechanical wear was the predominant mechanism. In the presence of additives, it was proven that a clearer synergistic effect between corrosion and wear was present. Lactic acid, despite not having a significant effect on tribocorrosion behavior of cp Ti, promoted slightly smaller and less worn surfaces as LA concentration increased. This phenomenon was attributed to probable oxidation reactions related to ejected wear debris, that provided a certain protection to cp Ti. In accordance, abrasion, adhesion and plastic deformation were detected for AS and AS+LA solutions, with the first showing more clearer signs of those wear mechanisms. For AS+PA solutions, on the other hand, a predominant lubricant effect was identified mainly do the visibly higher viscosity of these electrolytes (caused by the presence of P), which lead to the formation of considerably smaller wear tracks and lower wear volume loss. At OCP, a dangerous wear mechanism was observed, fatigue, which often takes place in well-lubricated contacts. At $+0.5V_{Ag/AgCl,}$ despite the formation of a potencial hybride layer, there were higher wear volume losses through possible enhancement of corrosion and wear triggered by this new surface layer.

Phosphoric acid had a significant effect and lactic acid did not, which means the hypothesis of this work was partially validated.

5.2 FUTURE WORKS

In order to have a more complete investigation, future works are required. Other additives, such as fluorides, hydrogen peroxide and citric acid should be investigated, so that comparisons could be drawn. Longer exposition time tests, to both electrolyte and mechanical action, could be performed since dental implants could be placed in the oral cavity for years. X-ray Photoelectron Spectroscopy (XPS) can be performed to obtain a quantitative and, therefore, more detailed analysis about the nature of oxide layers. Performance of EIS technique under applied anodic potentials, so that passive film growth mechanisms are clarified. And lastly, understand what surface treatments could be applied to cp Ti to improve its corrosion and tribocorrosion behavior for this specific application.

REFERENCES

[1] Instituto de Implantologia, Implantes dentários, (2021). https://www.institutodeimplantologia.pt/tratamentos/implantes-dentarios/ (accessed October 15, 2021).

[2] S.E. Eckert, S. Koka, The Bionic Human: Health Promotion for People With Implanted Prosthetic Devices, in: F.E. Johnson, K.S. Virgo, T.C. Laimore, R.A. Audisio (Eds.), The Bionic Human: Health Promotion for People With Implanted Prosthetic Devices. , 1st ed., Humana Press Inc., New Jersey, 2006: pp. 603–618.

[3] F.H. Froes, M. Qian, Titanium in Medical and Dental Applications, Woodhead Publishing, 2018.

[4] X. Liu, P.K. Chu, C. Ding, Surface modification of titanium, titanium alloys, and related materials for biomedical applications, Materials Science and Engineering: R: Reports. 47 (2004) 49–121.

[5] Instituto de Implantologia, Instituto de Implantologia no Diário de Notícias com artigo sobre saúde oral, (2018). https://www.institutodeimplantologia.pt/instituto-de-implantologia-no-diario-de-noticias-com-artigo-sobre-saude-oral/ (accessed October 15, 2021).

[6] B.D. Ratner, A.S. Hoffman, F.J. Schoen, J.E. Lemons, Biomaterials Science: An Introduction to Materials in Medicine, 1st ed., Academic Press, 1997.

[7] T. Fusayama, T. Katayori, S. Nomoto, Corrosion of Gold and Amalgam Placed in Contact with Each other, J Dent Res. 42 (1963) 1183–1197.

[8] J. Roscher, R. Holze, Corrosion of nonprecious metal alloys in dentistry in the presence of common saliva additives, Materials and Corrosion. 72 (2021) 1410–1416.

[9] M.W.J. Dodds, D.A. Johnson, C.K. Yeh, Health benefits of saliva: A review, J Dent. 33 (2005) 223–233.

[10] J.C.M. Souza, M. Henriques, W. Teughels, P. Ponthiaux, J.P. Celis, L.A. Rocha, Wear and Corrosion Interactions on Titanium in Oral Environment: Literature Review, J Bio Tribocorros. 1 (2015).

[11] R.L. Sakaguchi, J.M. Powers, Craig's Restorative Dental Materials , 13th ed., Elsevier Mosby, 2012.

[12] T. Liem, The orofacial structures, pterygopalatine ganglion and pharynx, Cranial Osteopathy. (2004) 437–484.

[13] F.H. Jones, Teeth and bones: applications of surface science to dental materials and related biomaterials, Surf Sci Rep. 42 (2001) 75–205.

[14] F. Schwarz, J. Derks, A. Monje, H.-L. Wang, Peri-implantitis, J Periodontol. 89 (2018) 267–290.

[15] T. Frisan, Bacterial genotoxins: The long journey to the nucleus of mammalian cells, Biochimica et Biophysica Acta (BBA) - Biomembranes. 1858 (2016) 567–575.

[16] C.W. Berry, T.J. Moore, C.A. Henry, M.J. Wagner, Antibacterial activity of dental implant metals, Implant Dent. 1 (1992) 59–65.

[17] R. Rajput, Z. Chouhan, S. Sundararajan, M. Sindhu, A Brief Chronological Review of Dental Implant History, International Dental Journal of Students Research. 4 (2016) 105–107.

[18] D.R. Scharf, D.P. Tarnow, Success Rates of Osseointegration for Implants Placed Under Sterile Versus Clean Conditions, J Periodontol. 64 (1993) 954–956.

[19] R.B. Osman, S. Ma, W. Duncan, R.K. de Silva, A. Siddiqi, M. v. Swain, Fractured zirconia implants and related implant designs: scanning electron microscopy analysis, Clin Oral Implants Res. 24 (2013) 592–597.

[20] J.B. Brunski, A.F. Moccia Jr., S.R. Pollack, E. Korostoff, D. Trachtenberg, Investigation of Surfaces of Retrieved Endosseous Dental Implants of Commercially Pure Titanium, in: H.A. Luckey, F. Kubli Jr. (Eds.), Titanium Alloys in Surgical Implants, ASTM STP 796, 1983: pp. 189–205.

[21] J.R. Dwek, The periosteum: what is it, where is it, and what mimics it in its absence?, Skeletal Radiolody. 39 (2010) 319–323.

[22] K. Leong, Biomaterials, Elsevier. (n.d.). https://www.sciencedirect.com/journal/biomaterials (accessed February 28, 2022).

[23] D.F. Williams, Implants in dental and maxillofacial surgery, Biomaterials. 2 (1981) 133–146.

[24] T. Albrektsson, M. Jacobsson, Bone-metal interface in osseointegration, J Prosthet Dent. 57 (1987) 597–607.

[25] M. Niiomi, M. Nakai, Titanium-Based Biomaterials for Preventing Stress Shielding between Implant Devices and Bone, Int J Biomater. (2011) 1–10.

[26] J.M. Tagliareni, E. Clarkson, Basic Concepts and Techniques of Dental Implants., Dent Clin North Am. 59 (2015) 255–264.

[27] J.E.G. González, J.C. Mirza-Rosca, Study of the corrosion behavior of titanium and some of its alloys for biomedical and dental implant applications, Journal of Electroanalytical Chemistry. 471 (1999) 109–115.

[28] D.W. Shoesmith, V.E. Annamalai, J.J. Noël, Corrosion of Titanium and Its Alloys, Reference Module in Materials Science and Materials Engineering. (n.d.).

[29] C.N. Elias, J.H.C. Lima, R. Valiev, M.A. Meyers, Biomedical applications of titanium and its alloy, JOM. 60 (2008) 46–49.

[30] D. Iijima, T. Yoneyama, H. Doi, H. Hamanaka, N. Kurosaki, Wear properties of Ti and Ti–6Al–7Nb castings for dental prostheses, Biomaterials. 24 (2003) 1519–1524.

[31] M. McCracken, Dental Implant Materials: Commercially Pure Titanium and Titanium Alloys, Journal of Prosthodontics. 8 (1999) 40–43.

[32] J.C. Wataha, Materials for endosseous dental implants, J Oral Rehabil. 23 (1996) 79–90.

[33] J.C.M. Souza, S.L. Barbosa, E. Ariza, J.-P. Celis, L.A. Rocha, Simultaneous degradation by corrosion and wear of titanium in artificial saliva containing fluorides, Wear. 292–293 (2012) 82–88.

[34] A.C. Vieira, A.R. Ribeiro, L.A. Rocha, J.-P. Celis, Influence of pH and corrosion inhibitors on the tribocorrosion of titanium in artificial saliva, Wear. 261 (2006) 994–1001.

[35] J.C.M. Souza, Biotribocorrosion behavior of titanium in simulated oral environments, Doctoral, University of Minho, 2010.

[36] J. Pouilleau, D. Devilliers, F. Garrido, S. Durand-Vidal, E. Mahé, Structure and Composition of Passive Titanium Oxide Films, Materials Science and Engineering. 47 (1997) 235–243.

[37] L.A. Rocha, F. Oliveira, H. v Cruz, C. Sukotjo, M.T. Mathew, Bio-tribocorrosion in dental applications, Bio-Tribocorrosion in Biomaterials and Medical Implants. (2013) 223–249.

[38] A.R.P. Ribeiro, Influence of pH and corrosion inhibitors on the tribocorrosion behaviour of titanium in different tribological geometries, Master, University of Minho, 2007.

[39] Q.L. Ma, L.Z. Zhao, R.R. Liu, B.Q. Jin, W. Song, Y. Wang, Y.S. Zhang, L.H. Chen, Y.M. Zhang, Improved implant osseointegration of a nanostructured titanium surface via mediation of macrophage polarization, Biomaterials. 35 (2014) 9853–9867.

[40] L. le Guéhennec, A. Soueidan, P. Layrolle, Y. Amouriq, Surface treatments of titanium dental implants for rapid osseointegration, Dental Materials. 23 (2007) 844–854.

[41] C. Rungsiyakull, Q. Li, G. Sun, W. Li, M. v Swain, Surface morphology optimization for osseointegration of coated implants, Biomaterials. 31 (2010) 7196–7204.

[42] L. Salou, A. Hoornaert, G. Louarn, P. Layrolle, Enhanced osseointegration of titanium implants with nanostructured surfaces: An experimental study in rabbits, Acta Biomater. 11 (2015) 494–502.

[43] L. Engelen, P.A.M. van den Keybus, R.A. de Wijk, E.C.I. Veerman, A.V.N. Amerongen, F. Bosman, J.F. Prinz, Andries van der Bilt, The effect of saliva composition on texture perception of semi-solids, Arch Oral Biol. 52 (2007) 518–25.

[44] P. Marsh, M. Martin, The Resident Oral Microflora, in: P. Marsh, M. Martin (Eds.), Oral Microbiology , 1st ed., Springer, New York, 1992: pp. 27–55.

[45] J.Luiz. Lorenzo, Microbiologia para o estudante de odontologia, (2004).

[46] V.A.R. Barão, M.T. Mathew, W.G. Assunção, J.C.-C. Yuan, M.A. Wimmer, C. Sukotjo, Stability of cp-Ti and Ti-6Al-4V alloy for dental implants as a function of saliva pH - an electrochemical study, Clin Oral Implants Res. 23 (2012) 1055–1062.

[47] G. Duffó, E.Q. Castillo, Development of an Artificial Saliva Solution for Studying the Corrosion Behavior of Dental Alloys, Corrosion. 60 (2004) 594–602.

[48] J.Y. Gal, Y. Fovet, M. Adib-Yadzi, About a synthetic saliva for in vitro studies, Talanta. 53 (2001) 1103–1115.

[49] J.M. Meyer, Corrosion resistance of nickel-chromium dental casting alloys, Corros Sci. 17 (1977) 971–982.

[50] J.M. Meyer, J.N. Nally, Influence of Artificial Salivas on the Corrosion of Dental Alloys, J Dent Res. 54 (1975) 678–681.

[51] M. Nakagawa, S. Matsuya, T. Shiraishi, M. Ohta, Effect of Fluoride Concentration and pH on Corrosion Behavior of Titanium for Dental Use, J Dent Res. 78 (1999) 1568–1572.

[52] A.J. de Gee, P. Pallav, Occlusal wear simulation with the ACTA wear machine, J Dent. 22 (1994) S21–S27.

[53] K.J. Anusavice, Mechanical Properties of Dental Materials, in: K.J. Anusavice, J. dos Santos, C. Shen (Eds.), Phillips' Science of Dental Materials, 11th ed., Elsevier, 2003: pp. 73–100.

[54] M. Sevimay, A. Usumez, G. Eskitascioglu, The influence of various occlusal materials on stresses transferred to implant-supported prostheses and supporting bone: A three-dimensional finite-element study, J Biomed Mater Res B Appl Biomater. 73 (2005) 140–147.

[55] C.E. Misch, Dental implant prosthetics, 2nd ed., Elsevier Mosby, 2005.

[56] M.G. Manda, P.P. Psyllaki, D.N. Tsipas, P.T. Koidis, Observations on an in-vivo failure of a titanium dental implant/abutment screw system: A case report, J Biomed Mater Res B Appl Biomater. 89 (2009) 263–273.

[57] D.G. Gratton, S.A. Aquilino, C.M. Stanford, Micromotion and dynamic fatigue properties of the dental implant–abutment interface, J Prosthet Dent. 85 (2001) 47–52.

[58] European Federation of Corrosion, Definition of corrosion, (2012). https://efcweb.org/efcweb/Working+Parties_Task+Forces/WP+Corrosion+Education/Definition+of+Corrosion.html (accessed November 24, 2021).

[59] C.E.B. Marino, L.H. Mascaro, EIS characterization of a Ti-dental implant in artificial saliva media: dissolution process of the oxide barrier, Journal of Electroanalytical Chemistry. 568 (2004) 115–120.

[60] G. Mabilleau, S. Bourdon, M.L. Joly-Guillou, R. Filmon, M.F. Baslé, D. Chappard, Influence of fluoride, hydrogen peroxide and lactic acid on the corrosion resistance of commercially pure titanium, Acta Biomater. 2 (2006) 121–129.

[61] K. Nakajo, S. Imazato, Y. Takahashi, W. Kiba, S. Ebisu, N. Takahashi, Fluoride released from glass-ionomer cement is responsible to inhibit the acid production of caries-related oral streptococci, Dental Materials. 25 (2009) 703–708.

[62] N. Schiff, B. Grosgogeat, M. Lissac, F. Dalard, Influence of fluoride content and pH on the corrosion resistance of titanium and its alloys, Biomaterials. 23 (2002) 1995–2002.

[63] M.E.P. Souza, L. Lima, C.R.P. Lima, C.A.C. Zavaglia, C.M.A. Freire, Effects of pH on the electrochemical behaviour of titanium alloys for implant applications, J Mater Sci Mater Med. 20 (2009) 549–552.

[64] J.C.M. Souza, S.L. Barbosa, E.A. Ariza, M. Henriques, W. Teughels, P. Ponthiaux, J.P. Celis, L.A. Rocha, How do titanium and Ti6Al4V corrode in fluoridated medium as found in the oral cavity? An in vitro study, Materials Science and Engineering: C. 47 (2015) 384–393.

[65] M. Koike, H. Fujii, In vitro assessment of release from titanium by immersion tests, J Prosthodont Res. 41 (1997) 675–679.

[66] M. Koike, H. Fujii, In vitro assessment of corrosive properties of titanium as a biomaterial, J Oral Rehabil. 28 (2001) 540–548.

[67] M. Koike, H. Fujii, The corrosion resistance of pure titanium in organic acids, Biomaterials. 22 (2001) 2931–2936.

[68] Q. Qu, L. Wang, Y. Chen, L. Li, Y. He, Z. Ding, Corrosion Behavior of Titanium in Artificial Saliva by Lactic Acid, Materials. 7 (2014) 5528–5542.

[69] S.P. Kedici, A.A. Aksüt, M.A. Kílíçarslan, G. Bayramoğlu, K. Gökdemir, Corrosion behaviour of dental metals and alloys in different media, J Oral Rehabil. 25 (1998) 800–808.

[70] A.A. Ghoneim, A.S. Mogoda, K.A. Awad, F. Heakal, Electrochemical Studies of Titanium and its Ti-6Al-4V Alloy in Phosphoric Acid Solutions, Int J Electrochem Sci. 7 (2012) 6538–6554.

[71] P. Ponthiaux, F. Wenger, D. Drees, J.P. Celis, Electrochemical techniques for studying tribocorrosion processes, Wear. 256 (2004) 459–468.

[72] S. Mischler, EFC Working Party 18: Tribo-corrosion, European Federation of Corrosion. (2019). https://efcweb.org/efcweb/Working+Parties_Task+Forces/WP+Tribo_Corrosion-p-104114.html (accessed November 28, 2021).

[73] S. Mischler, S. Debaud, D. Landolt, Wear-Accelerated Corrosion of Passive Metals in Tribocorrosion Systems, J Electrochem Soc. 145 (1998) 750–758.

[74] D. Landolt, S. Mischler, M. Stemp, Electrochemical methods in tribocorrosion: a critical appraisal, Electrochim Acta. 46 (2001) 3913–3929.

[75] J.-P. Celis, P. Ponthiaux, Definition of tribocorrosion and its importance, in: J.-P. Celis, P. Ponthiaux (Eds.), Testing Tribocorrosion of Passivating Materials Supporting Research and Industrial Innovation: Handbook, 1st ed., Maney Publishing, 2012: pp. 1–13.

[76] A. Siddaiah, A. Kasar, R. Ramachandran, P.L. Menezes, Introduction to tribocorrosion, Tribocorrosion: Fundamentals, Methods, and Materials. (2021) 1–16.

[77] T.S.N.S. Narayanan, Nanocoatings to improve the tribocorrosion performance of materials, Corrosion Protection and Control Using Nanomaterials. (2012) 167–212.

[78] S. Barril, N. Debaud, S. Mischler, D. Landolt, A tribo-electrochemical apparatus for in vitro investigation of fretting–corrosion of metallic implant materials, Wear. 252 (2002) 744–754.

[79] H. Cruz, J. Souza, M. Henriques, L. Rocha, Tribocorrosion and Bio-Tribocorrosion in the Oral Environment: The Case of Dental Implants, in: Biomedical Tribology, 2011: p. 33.

[80] D. Landolt, Electrochemical and materials aspects of tribocorrosion systems, J Phys D Appl Phys. 39 (2006) 3121–3127.

[81] F. Al-Sanabani, A. Madfa, N. Al-Qudaimi, Alumina ceramic for dental applications: A review article, American Journal of Materials Research. 1 (2014) 26–34.

[82] M.J. Neale, Wear mechanisms, Lubrication and Reliability Handbook. (2001) 1–3.

[83] S. Kumar, T.S.N.S. Narayanan, S.G.S. Raman, S.K. Seshadri, Surface modification of CP-Ti to improve the fretting-corrosion resistance: Thermal oxidation vs. anodizing, Materials Science and Engineering: C. 30 (2010) 921–927.

[84] S. Mischler, Triboelectrochemical techniques and interpretation methods in tribocorrosion: A comparative evaluation, Tribol Int. 41 (2008) 573–583.

[85] M.T. Mathew, S. Abbey, N.J. Hallab, D.J. Hall, C. Sukotjo, M.A. Wimmer, Influence of pH on the tribocorrosion behavior of CpTi in the oral environment: synergistic interactions of wear and corrosion, J Biomed Mater Res B Appl Biomater. 100 (2012) 1662–1671.

[86] H.J. Busscher, M. Rinastiti, W. Siswomihardjo, H.C. van der Mei, Biofilm formation on dental restorative and implant materials, J Dent Res. 89 (2010) 657–665.

[87] J.C.M. Souza, M. Henriques, R Oliveira, W. Teughels, J.-P. Celis, L.A. Rocha, Do oral biofilms influence the wear and corrosion behavior of titanium?, Biofouling. 26 (2010) 471–478.

[88] X. Chen, K. Shah, S. Dong, L. Peterson, E. Callagon La Plante, G. Sant, Elucidating the corrosion-related degradation mechanisms of a Ti-6Al-4V dental implant, Dental Materials. 36 (2020) 431–441.

[89] A.I. Costa, L. Sousa, A.C. Alves, F. Toptan, Tribocorrosion behaviour of bio-functionalized porous Ti surfaces obtained by two-step anodic treatment, Corros Sci. 166 (2020) 108467.

[90] L. Sousa, A.R. Mendes, A.M.P. Pinto, F. Toptan, A.C. Alves, Influence of Calcium Acetate Concentration in Electrolyte on Tribocorrosion Behaviour of MAO Treated Titanium, Metals (Basel). 11 (2021).

[91] I. Çaha, A.C. Alves, P.A.B. Kuroda, C.R. Grandini, A.M.P. Pinto, L.A. Rocha, F. Toptan, Degradation behavior of Ti-Nb alloys: Corrosion behavior through 21 days of immersion and tribocorrosion behavior against alumina, Corros Sci. 167 (2020) 108488.

[92] A.C. Alves, F. Wenger, P. Ponthiaux, J.P. Celis, A.M. Pinto, L.A. Rocha, J.C.S. Fernandes, Corrosion mechanisms in titanium oxide-based films produced by anodic treatment, Electrochim Acta. 234 (2017) 16–27.

[93] V.B. Singh, S.M.A. Hosseini, The electrochemical and corrosion behaviour of titanium and its alloy (VT-9) in phosphoric acid, Corros Sci. 34 (1993) 1723–1732.

[94] R.M. Souto, M.M. Laz, R.L. Reis, Degradation characteristics of hydroxyapatite coatings on orthopaedic TiAlV in simulated physiological media investigated by electrochemical impedance spectroscopy, Biomaterials. 24 (2003) 4213–4221.

[95] I. Çaha, A.C. Alves, C. Chirico, A.M. Pinto, S. Tsipas, E. Gordo, F. Toptan, Improved tribocorrosion behavior on bio-functionalized β-type titanium alloy by the pillar effect given by TiN reinforcements, Surf Coat Technol. 415 (2021) 127122.

[96] W. Xu, A. Yu, X. Lu, M. Tamaddon, L. Ng, M. Dilawer Hayat, M. Wang, J. Zhang, X. Qu, C. Liu, Synergistic interactions between wear and corrosion of Ti-16Mo orthopedic alloy, Journal of Materials Research and Technology. 9 (2020) 9996–10003.

[97] J.C.J. Bart, E. Gucciardi, S. Cavallaro, Formulating lubricating oils, Biolubricants. (2013) 351–395.

[98] T. Hanawa, K. Asami, K. Asaoka, Repassivation of titanium and surface oxide film regenerated in simulated bioliquid, J Biomed Mater Res. 40 (1998) 530–538.

[99] Z. Doni, A.C. Alves, F. Toptan, J.R. Gomes, A. Ramalho, M. Buciumeanu, L. Palaghian, F.S. Silva, Dry sliding and tribocorrosion behaviour of hot pressed CoCrMo biomedical alloy as compared with the cast CoCrMo and Ti6Al4V alloys, Materials & Design (1980-2015). 52 (2013) 47–57.

[100] A.C. Alves, F. Oliveira, F. Wenger, P. Ponthiaux, J.-P. Celis, L.A. Rocha, Tribocorrosion behaviour of anodic treated titanium surfaces intended for dental implants, J Phys D Appl Phys. 46 (2013) 404001.

[101] S. Barril, S. Mischler, D. Landolt, Electrochemical effects on the fretting corrosion behavior of Ti6Al4V in 0.9% sodium chloride solution, Wear. 259 (2005) 282–291.

[102] J.R. Gomes, Noções de Tribologia - Desgaste, (2021) 19–22.

[103] G.W. Stachowiak, A.W. Batchelor, 14 Fatigue Wear, Tribology Series. 24 (1993) 657–681.

[104] F. Toptan, A.C. Alves, Ó. Carvalho, F. Bartolomeu, A.M.P. Pinto, F. Silva, G. Miranda, Corrosion and tribocorrosion behaviour of Ti6Al4V produced by selective laser melting and hot pressing in comparison with the commercial alloy, J Mater Process Technol. 266 (2019) 239–245.

[105] L. Zhang, Y. Duan, R. Gao, J. Yang, K. Wei, D. Tang, T. Fu, The Effect of Potential on Surface Characteristic and Corrosion Resistance of Anodic Oxide Film Formed on Commercial Pure Titanium at the Potentiodynamic-Aging Mode, Materials (Basel). 12 (2019) 370.

[106] J.I. Silva, A.C. Alves, A.M. Pinto, F. Toptan, Corrosion and tribocorrosion behavior of Ti–TiB–TiNx in-situ hybrid composite synthesized by reactive hot pressing, J Mech Behav Biomed Mater. 74 (2017) 195–203.